



1074377

## Accepted Manuscript

Overview of the Mineralogy of the Biwabik Iron Formation, Mesabi Iron Range,  
Northern Minnesota

Peter L. McSwiggen, G.B. Morey

PII: S0273-2300(07)00135-3  
DOI: [10.1016/j.yrtph.2007.09.010](https://doi.org/10.1016/j.yrtph.2007.09.010)  
Reference: YRTPH 2051

To appear in: *Regulatory Toxicology and Pharmacology*

Received Date: 13 September 2007  
Accepted Date: 26 September 2007



Please cite this article as: McSwiggen, P.L., Morey, G.B., Overview of the Mineralogy of the Biwabik Iron Formation, Mesabi Iron Range, Northern Minnesota, *Regulatory Toxicology and Pharmacology* (2007), doi: [10.1016/j.yrtph.2007.09.010](https://doi.org/10.1016/j.yrtph.2007.09.010)

This is a PDF file of an unedited manuscript that has been accepted for publication. As a service to our customers we are providing this early version of the manuscript. The manuscript will undergo copyediting, typesetting, and review of the resulting proof before it is published in its final form. Please note that during the production process errors may be discovered which could affect the content, and all legal disclaimers that apply to the journal pertain.

# Overview of the Mineralogy of the Biwabik Iron Formation, Mesabi Iron Range, Northern Minnesota

Peter L. McSwiggen<sup>a,\*</sup> and G.B. Morey<sup>b</sup>

<sup>a, b</sup> *McSwiggen & Associates, 2855 Anthony Lane South, Suite B1, St. Anthony, MN 55418*

\* Corresponding author. Phone: +1 612 781 2282

Fax: +1 612 781 7540

*E-mail address:* pmcs@mcswiggenassoc.com (Peter L. McSwiggen)

## Abstract

The mineralogy of the Biwabik Iron Formation changes dramatically from west to east as the formation nears the basal contact of the Duluth Complex. This reflects a contact metamorphism that took place with the emplacement of the igneous Duluth Complex at temperatures as high as 1200°C. However, the mineralogy of the Biwabik Iron Formation also varies vertically through the stratigraphy of the unit. This variability in both the vertical and horizontal dimensions makes it difficult to predict exact horizons where specific minerals will occur. The iron-formation has been subdivided into four broad stratigraphic units (lower cherty, lower slaty, upper cherty, and upper slaty) and into four lateral mineralogical zones (1-4). Zone 1, the westernmost zone, is characterized by quartz, magnetite, hematite, carbonates, talc, chamosite, greenalite, minnesotaite and stilpnomelane. The silicate mineralogy in Zone 2 of the Biwabik Iron Formation changes very little. However, the minerals begin to change dramatically in Zone 3. Most significantly, Zone 3 is characterized by the appearance of grunerite in both a tabular form and a fibrous form. In Zone 4, the original silicate minerals have completely reacted, and a new suite of minerals occupies the iron-formation. These include grunerite, hornblende, hedenbergite, ferrohypersthene (ferrosilite), and fayalite.

**Keywords:** Biwabik Iron Formation; Duluth Complex; mineralogy

## 1. Introduction

The Biwabik Iron Formation occurs as a northeast-trending outcrop belt, 2.5 to 3.0 miles wide and 122 miles long (Fig. 1A). The outcrop belt defines the "Mesabi Iron Range", a world-class iron-ore deposit. Over 3.5 billion tons of ore have been shipped from the range. Much has been written about the magnetite and its transformation into taconite ore, but less information is available concerning other components in the iron-formation that typically end up in the over 7 billion tons of waste materials commonly referred to as tailings. This report focuses on the mineralogy of those parts of the Biwabik Iron Formation.

## 2. Regional setting

As described by Jirsa et al. (this volume), the Biwabik Iron Formation is underlain by a thin basal quartz arenitic sequence called the Pokegama Quartzite and overlain by a thick graywacke-

shale sequence named the Virginia Formation (Fig. 1B). Contacts between the iron-formation and underlying and overlying clastic strata are conformable and gradational. Strata within the Biwabik have been classified by texture into two fundamentally different kinds of iron-formation; (1) cherty materials, which are seemingly coarse-grained, thick bedded, and typically, but not always, rich in quartz and iron oxides, and (2) slaty materials, which are generally fine-grained, finely laminated to very thin bedded, and composed mostly of iron silicates and iron carbonates. Beds or groups of beds having cherty or slaty attributes are interlayered on all scales. Despite the heterogeneity, the Biwabik can be divided into four lithostratigraphic entities, which are from bottom to top, (1) Lower Cherty, (2) Lower Slaty, (3) Upper Cherty, and (4) Upper Slaty. Wolff (1917) originally defined these entities and coined them "divisions", and this usage is still adhered to by some of the mining companies operating along the range. Subsequent studies by White (1954) showed that the divisions were mappable entities and therefore have been considered as members.

Most of the Biwabik Iron Formation has not been metamorphosed to any extent and contains mineral assemblages indicative of low-grade diagenetic processes (Morey, 2003). However, on the east end of the range, a thermal metamorphic event associated with the emplacement of the Duluth Complex produced a metamorphic aureole some 2-3 miles wide. Although quartz and magnetite-bearing assemblages within the aureole were thoroughly recrystallized and although a significant number of metamorphic silicates, such as grunerite-cummingtonite, fayalite, ferrohypersthene, hedenbergite, hornblende, and actinolite, were produced, the cherty and slaty members and their associated attributes can still be recognized.

### 3. Petrographic overview

French (1968) provided a broad overview of the iron-formation at the east end of the range. He distinguished a broad zone of "unmetamorphosed" iron-formation, his Zone 1, and three metamorphic zones marked by mineralogic changes along the strike of the iron-formation toward the contact with rocks of the Duluth Complex. Zone 2 includes transitional taconite, Zone 3, moderately metamorphosed taconite, and Zone 4, highly metamorphosed taconite.

Comparatively, little information regarding mineralogic aspects of the iron-formation in Zone 1 has been published since the work of Gruner (1946) and French (1968; 1973). In contrast, various aspects of the metamorphic aureole have been described extensively by Gundersen (1960), Gundersen and Schwartz (1962), French (1968), Griffin and Morey (1969), Bonnichsen (1969; 1975) and Morey and others (1972). According to Gundersen and Schwartz (1962), the thermal metamorphic processes associated with emplacement of the Duluth Complex were manifested largely by simple recrystallization and the development of fayalite, magnetite, and quartz-bearing assemblages. Assemblages containing other metamorphic silicates formed by metasomatic processes involving the injection of magnesium- and calcium-bearing igneous solutions. Subsequent workers however, view mineralogic change as being essentially isochemical except for the loss of water and carbon dioxide.

### 4. Zone 1: unmetamorphosed iron formation

Unmetamorphosed iron-formation of Zone 1 is characterized by textural attributes strikingly similar to those associated with limestone of the Phanerozoic age. The basic distinction between cherty and slaty varieties of iron-formation is one that has been recognized for a long time by geologists studying the Biwabik Iron Formation (Wolff, 1917). Mengel (1965) recognized that

the cherty varieties are marked by sand-size grains, locally called granules, but including pebbles of admixed chert and carbonates, angular fragments of algal structures, ooids, oncolites, and detrital quartz and feldspar. The admixed material commonly occurs in strata having graded bedding or cross bedding showing that the clasts behaved as particulate detritus as in arenaceous clastic rocks. On the other hand, LaBerge (1967) showed that the slaty varieties have textural attributes similar in many respects to those in siltstone or shale.

Textural elements in cherty strata include; (1) granules, (2) oolites and pisoliths, (3) oncolites, and (4) cements. Granules greatly predominate over the other kinds of clasts that are generally associated with intergranular cement. Most granules are internally structureless. They range in length from about 0.5 mm to 1 mm and are irregularly rounded or ovoid in shape. The granules typically consist of extremely fine grained monomineralic or polymineralic aggregates. Boundaries between granules and cement are typically sharp, but may be diffuse because of recrystallization. Many granules commonly exhibit fractures that represent shrinkage or syneresis cracks presumably formed by expulsion of water from a gel.

Although they differ in size, oolites and pisoliths are typically concentrically laminated. Some oolites have only a few concentric rims and are akin to structures in limestone known as superficial oolites. Other oolite, grapestones, are formed from clusters or aggregates of smaller oolites or granules held together by concentric rims that impart an overall botryoidal shape. Still other oolites have eccentric rims suggestive of an oncolite origin. Regardless, oolites and pisoliths are formed *in situ* by a combination of chemical and physical processes.

Distinctly different rim and pore cements are a marked feature of the cherty rocks. Older rim cement generally consist of fine-grained fibrous or bladed chert oriented perpendicular to the surfaces of the granules or oolites. This cement is paragenetically followed by pore-filling quartz that typically is blocky and coarse-grained.

Textural relationships in slaty varieties of iron-formation are complex and difficult to interpret because of the generally fine grain size of the constituent minerals. The principal textural elements include varying proportions of very fine-grained chert, carbonate or iron silicate. A few less well defined textural elements may include possible volcanic shards.

Matrices in slaty rocks differ from cements in cherty rocks only in their presumed mode of origin. Matrices were probably deposited *in situ* as ooze or muds whereas cements were precipitated in interstitial voids after granules and oolites were deposited. Consequently, matrices tend to occur as thin, undisturbed laminae that have regular-sharp contacts. However, isolated granules are not uncommon, particularly in matrices dominated by chert.

#### 4.1. Mineral associations

Particular stratigraphic units in Drill Hole 1 (see location map, Fig. 1A) have distinct mineral associations that may in some cases approximate mineral assemblages (Fig. 2). Shaly rocks of the Virginia Formation are dominated by a sepioclorite (chamosite) + sericite  $\pm$  albitic plagioclase  $\pm$  quartz. Slaty rocks in the uppermost part of the Upper Slaty interval consist predominantly of calcite  $\pm$  dolomite  $\pm$  chamosite  $\pm$  stilpnomelane  $\pm$  quartz  $\pm$  an iron oxide, mainly magnetite. Iron-formation a few feet below the transition contains siderite  $\pm$  ankerite  $\pm$  chamosite  $\pm$  stilpnomelane  $\pm$  quartz  $\pm$  an iron oxide, mainly hematite. Magnetite appears to be confined to scattered beds or laminae. Rocks assigned to the Upper Cherty interval contain chamosite  $\pm$  stilpnomelane  $\pm$  siderite  $\pm$  quartz  $\pm$  hematite, along with scattered thin beds of monomineralic magnetite. Lower Slaty beds also consist predominantly of chamosite  $\pm$  stilpnomelane  $\pm$  siderite  $\pm$  quartz, but appear to lack a discrete iron oxide phase. Chamosite

disappears from the upper part of the Lower Cherty interval and is replaced by minnesotaite  $\pm$  talc. Other mineral phases include stilpnomelane  $\pm$  siderite  $\pm$  ankerite  $\pm$  quartz  $\pm$  iron oxide (hematite). Midway in the member, stilpnomelane disappears and the strata are dominated by minnesotaite  $\pm$  talc  $\pm$  siderite  $\pm$  ankerite  $\pm$  quartz. Ultimately talc disappears and typical mineral associations contain greenalite  $\pm$  minnesotaite  $\pm$  siderite  $\pm$  ankerite  $\pm$  quartz  $\pm$  hematite. The basal red taconite consists of chert  $\pm$  hematite  $\pm$  chamosite  $\pm$  ankerite. Grains of detrital quartz and potassium feldspar are scattered throughout the interval. Quartz and potassium feldspar  $\pm$  greenalite  $\pm$  calcite define mineral associations in quartz arenitic strata typical of the Pokegama Quartzite.

#### 4.2. Quartz and chert

The most abundant mineral in the iron-formation in Drill Hole 1 is quartz. It is by far the dominant constituent of granules, oolites, and pisoliths, cements, and matrices. Morphological varieties include microcrystalline quartz (micritic quartz), fibrous quartz (chalcedony), and coarse-grained quartz (megaquartz). Some of the micritic quartz has undergone considerable recrystallization.

Most granules consist entirely of micritic quartz or of micritic quartz admixed with lesser amounts of silicates, carbonates or iron oxides. Chalcedony, or less commonly, megaquartz, fills internal shrinkage cracks and fractures. Early chalcedonic cement typically forms a radial fringe surrounding many of the intraclasts. Chalcedonic rim cement is followed paragenetically by pore-filling cement consisting mostly of megaquartz.

In slaty iron-formation, micritic quartz occurs within layers admixed with various proportions of iron silicates or less commonly as monomineralic laminae. Many such laminae are content graded and pass into silicate- and carbonate-rich layers as the proportions of these phases increases.

#### 4.3. Silicate minerals

##### 4.3.1. Chamosite and greenalite

Since the silicates in unmetamorphosed iron-formation have not been described previously in any detail, their morphological and chemical attributes are discussed in the following sections. Figure 3A-D shows that the compositions of individual phases deviate substantially from the ideal compositions reported in the literature.

Pale-green chamosite is a widely distributed phase in Drill Hole 1. It occurs within both granules and oolites as rim cement and matrix material between granules (Fig. 4). Chamosite also pseudomorphically replaces shard-like structures of possible volcanic origin found within thinly layered packets of slaty iron-formation scattered about within thicker intervals of cherty iron-formation. Similar shard-like structures, also involving chamosite, occur within silicate-bearing carbonate laminae in stratigraphic intervals dominated by slaty varieties of iron-formation.

Ideal chamosite  $[\text{Fe}_6(\text{Al},\text{Si})_4\text{O}_{10}(\text{OH})_8]$  is an iron chlorite. It differs mainly from greenalite in containing larger amounts of alumina (Fig. 5). Although chamosite in Drill Hole 1 has a variety of habits, average microprobe analyses are broadly similar and approximate the average composition of chamosite found in Phanerozoic ironstone (Klein, 1983). Chamosite in the Upper

Slaty differs mainly in having somewhat more  $\text{Al}_2\text{O}_3$  and  $\text{MgO}$ . However, in the Upper Cherty, the chamosite composition has changed considerably and the  $\text{Mg/Fe}$  ratio is now about 50:50. In the Lower Slaty, chamosite contains more Fe than Mg whereas in the Lower Cherty it is more Mg rich.

Greenalite is restricted to the Lower Cherty where it has textural attributes similar to those of chamosite. Most greenalite-bearing granules are aggregates of bright green, pale green or pale brown material typically intergrown with micritic quartz, stilpnomelane, and minor minnesotaite. Many oolites have cores that are composed primarily of greenalite and rimmed by greenalite interlayered with chalcedonic quartz.

According to Gruner (1936), the structure of greenalite  $[\text{Fe}_6\text{Si}_4\text{O}_{10}(\text{OH})_8]$  is the ferrous analog of antigorite  $[\text{Mg}_6\text{Si}_4\text{O}_{10}(\text{OH})_8]$ . It always contains at least some magnesium. Variations in composition are illustrated graphically in Fig. 6. Many of the analyzed samples lie close to the ideal greenalite composition; substitutions are minor and typically involve replacement of  $\text{FeO}$  and  $\text{SiO}_2$  by small quantities of  $\text{MgO}$  and  $\text{Al}_2\text{O}_3$  respectively. However, some samples contain almost 8 wt. percent  $\text{Al}_2\text{O}_3$  and tend to plot along a join line that extends between an ideal greenalite composition and an ideal chamosite composition. Even single granules contain variable quantities of  $\text{Al}_2\text{O}_3$  and there appears to be a correlation between  $\text{Al}_2\text{O}_3$  content and color. Bright green greenalite typically contains 5 wt. percent or less  $\text{Al}_2\text{O}_3$ ; pale green to pale brown greenalite contains 4.8 to 6.3 wt. percent  $\text{Al}_2\text{O}_3$  whereas dark brown granules contain 7.0 to 7.8 wt. percent  $\text{Al}_2\text{O}_3$ . According to Klein (1974), typical greenalite should contain no more than around 5 wt. percent  $\text{Al}_2\text{O}_3$ . He suggests that some of the greenalite having 6 to nearly 8 wt. percent  $\text{Al}_2\text{O}_3$  may in fact be berthierine, a  $7\text{\AA}$  chamosite. Careful X-ray work will be needed to determine if the alumina-rich phases reported here are indeed berthierine ( $7\text{\AA}$ ), or chamosite ( $7\text{\AA}$ ), or an iron-rich chloride ( $14\text{\AA}$ ).

Since the chamosite analyzed in this study has a composition that lies along a join line between greenalite and chamosite, it is clear that the two phases are structurally related. Given that the two have similar paragenetic histories, it is likely that chamosite served as a sink for alumina and the two therefore reflect heterogeneities in bulk composition.

#### 4.3.2. *Minnesotaite*

Minnesotaite is a minor constituent; mainly in granules admixed, with greenalite (Fig. 7), or with greenalite and stilpnomelane. It is somewhat more abundant in slaty varieties where it is associated with stilpnomelane.

Pale brownish-green to colorless minnesotaite occurs as felt-like masses or as fine- to medium-grained acicular crystals arranged in sprays of acicular bundles (Fig. 7) or "bowties". Both habits are scattered haphazardly, but the bowties especially occur along the greenalite granules (Fig. 8). Felt-like, disseminated masses of greenalite and minnesotaite also seem to replace micritic chert, both in granules and in matrix material. Many granules of minnesotaite are fractured, and the fractures are filled with chalcedonic quartz (Fig. 9).

Minnesotaite  $[\text{Fe}_3\text{Si}_4\text{O}_{10}(\text{OH})_2]$  is the iron analog of talc  $(\text{Mg}_3\text{Si}_4\text{O}_{10}(\text{OH})_2)$ , although the two have different structures. It differs from greenalite in containing more silica, but like greenalite and chamosite, it always contains some magnesium. In Drill Hole 1, it differs from an ideal end-member composition in containing almost 6 wt. percent  $\text{MgO}$ .

#### 4.3.3. *Talc*

Talc occurs in the Lower Cherty division, almost always intergrown with minnesotaite. It has a habit similar to minnesotaite, but tends to be more sheaf-like. Microprobe analyses (Fig. 10) yield compositions intermediate between ideal talc [ $\text{Mg}_3\text{Si}_4\text{O}_{10}(\text{OH})_2$ ] and minnesotaite [ $\text{Fe}_3\text{Si}_4\text{O}_{10}(\text{OH})_2$ ] implying either the presence of ferroan talc (Miyano, 1978) or the presence of intimately admixed talc and minnesotaite.

#### 4.3.4. *Stilpnomelane*

Stilpnomelane is a typically cryptocrystalline, highly pleochloric (yellowish brown to dark brown) sheaf-like silicate found in a variety of textural settings. Commonly, it has a pale brown or reddish brown color, but some varieties have a greenish brown color. The range of colors implies a range of  $\text{Fe}^{+2}/(\text{Fe}^{+2} + \text{Fe}^{+3})$  ratios on a microscopic scale.

Although granules composed entirely of stilpnomelane may occur (Fig. 11), stilpnomelane more commonly occurs as individual laths (Fig. 12) or radiating sheaves (Fig. 13) in subordinate amounts within granules of micritic chert or carbonate (Fig. 14). Crosscutting relationships imply that the stilpnomelane is the youngest phase. It is noteworthy that many stilpnomelane-bearing granules are broken by shrinkage cracks that are filled with chalcedony. The stilpnomelane must be an early-formed diagenetic phase. Rarely, stilpnomelane also may be found within the cores of oolites along with fine-grained chamosite and minnesotaite. Monomineralic rims of stilpnomelane surround many of these oolites. The oolites also are cut by chalcedony-filled shrinkage cracks.

Lastly, granules of admixed stilpnomelane and micritic chert may be found floating within siderite, either as matrix or as cement. Margins of the granules have been partially replaced by the siderite, implying that it is paragenetically later than phases within the granules.

Stilpnomelane in slaty varieties of iron-formation is not easily discernable because of a very fine grain size and a semi-opaque nature of many of the individual layers. In places, it occurs as circular grains ("microgranules") set within a felt-like matrix of admixed minnesotaite and greenalite. Stilpnomelane also appears to replace elongate shard-like structures of possible volcanic origin embedded within a siderite matrix. There it generally forms cryptocrystalline aggregates that have preferred orientations perpendicular to shard boundaries.

The composition of stilpnomelane is more complex than that of greenalite or minnesotaite, mainly in containing small and variable, but essential, amounts of  $\text{K}_2\text{O}$  and  $\text{Na}_2\text{O}$ , as well as larger amounts of  $\text{Al}_2\text{O}_3$  (Fig. 15).

Although the structure of stilpnomelane has not been fully established, Gruner (1944) suggested that it is fundamentally talc-like. Similarly, a precise chemical formula remains uncertain; nonetheless, albeit an incorrect simplified formula is useful for comparative purposes [ $(\text{Ca}, \text{Na}, \text{K}) (\text{Fe}, \text{Mg})_3\text{S}_{14}\text{O}_{10}(\text{OH})_2$ ]. Many of the analyzed samples have that approximate composition (Fig. 15). However, some analyzed grains have compositions along a mixing line that extends between stilpnomelane and chamosite. These two phases are either structurally related or are finely intergrown. Similarly in one sample, a stilpnomelane-like phase appears to be admixed with two other phases, an alumina-poor chamosite, and an unidentified phase that is both silica-rich and alumina-rich. Although it is possible that the analyzed silica values reflect the presence of very fine chert, that alone would not explain the atypical alumina values. Additional analyses did nothing to clarify this point.

#### 4.4 *Carbonate minerals*

Samples of both cherty and slaty varieties of iron-formation contain three or four carbonate species: calcite, siderite, and members of the dolomite-ankerite and the kutnahorite/ferroan kutnahorite series (Fig. 16).

#### 4.4.1. Siderite

Siderite ( $\text{FeCO}_3$ ) occurs in cherty varieties of iron-formation in several ways. Primary siderite occurs in granules as aggregates of rounded to anhedral grains cemented together by rhombic overgrowths (Fig. 14). Many of the rounded grains have spherulitic structures and are set in coarsely crystalline siderite marked by interlocking rounded and rhombic grains. Textural relationships imply that the granules and the enclosing matrix are more-or-less contemporaneous in origin.

Secondary siderite occurs as coarse, zoned and/or twinned rhombohedra that replace granules composed of micritic chert and their associated cements. Relict granules form ghosts that are preserved within grains of rhombic siderite. Secondary siderite also occurs in mottled areas as aggregates of fine-grained anhedral grains. The mottles enclose phases such as chert and the several iron silicates.

Siderite in slaty varieties of iron-formation typically occurs as small spheres cemented together by rhombic overgrowths. The spheres have cryptocrystalline cores that are turbid or semi-opaque. Individual carbonate-rich laminae may consist entirely of spherical siderite or of spherical siderite and associated rhombic overgrowths, or entirely of interlocking rhombic grains. Rhombic siderite also occurs as disseminated grains in calcite-rich laminae. The two phases are more-or-less contemporaneous. Other carbonate-rich laminae are typically interlayered with dark-colored greenalite or stilpnomelane-rich laminae that have various proportions of admixed spherical siderite. Many of these laminae are recrystallized as evidenced by patchy mixtures of fine-grained silicates and granoblastic clusters of rhombohedral or subhedral siderite.

The composition of siderite can be expressed in terms of four components:  $\text{FeCO}_3$ ,  $\text{MnCO}_3$ ,  $\text{MgCO}_3$ , and  $\text{CaCO}_3$ , which are in solid solution. Some samples from the Lower Cherty division contain as much as 20 to 25 mole percent  $\text{MnCO}_3$  (Fig. 17). Microprobe analyses from the Upper Slaty, Upper Cherty, and Lower Slaty divisions (Fig. 17) are broadly similar, and average around  $\text{Fe}_{.88-.84}\text{Mg}_{.03-.11}\text{Ca}_{.02-.03}\text{Mn}_{.02-.07}\text{CO}_3$ . Some substitution of Fe by Mg occurs locally, and most samples contain <5 wt. percent  $\text{MnCO}_3$ , but a few samples from the Upper Cherty division contain as much as 10 wt. percent  $\text{MnCO}_3$ , generally at the expense of  $\text{MgCO}_3$ .

These measured compositions are considerably more iron-rich than an average composition of 68 to 83 mole percent  $\text{FeCO}_3$  (French, 1968). In contrast, the average composition of siderite from the Lower Cherty (Fig. 17) differs considerably from that of the remainder of the iron-formation. There, both magnesium and manganese substitute for iron yielding an average composition of  $(\text{Fe}_{.60-.78}\text{Mg}_{.15-.19}\text{Ca}_{.02-.03}\text{Mn}_{.04-.22})\text{CO}_3$ .

#### 4.4.2. Dolomite-ankerite series

Pure dolomite [ $\text{CaMg}(\text{CO}_3)_2$ ] has a restricted stratigraphic distribution in the transitional interval between the Biwabik and Virginia formations. Much of it has a coarse replacement texture marked by euhedral rhombic crystals that are considerably zoned. Microprobe analyses show that the dolomite has a composition with little or no substitution of FeO or MnO, and has an average composition of  $(\text{Ca}_{.54}\text{Mg}_{.41}\text{Fe}_{.04}\text{Mn}_{.01})\text{CO}_3$ .

Ankerite  $[\text{Ca}(\text{Mg},\text{Fe})(\text{CO}_3)_2]$ , in contrast to dolomite, is widely distributed and occurs in both cherty and slaty varieties of iron-formation. It typically forms coarse-grained rhombs that can be extensively zoned (Fig. 18). Replacement by ankerite of earlier-formed phases commonly develops patches of aggregated grains, which give the rocks a mottled appearance. In some samples, the mottles contain remnants of earlier granules, which are outlined by fine masses of later growth (Fig. 19).

Ankerite rarely occurs in carbonate-rich slaty layers where it forms irregular beds and patches of anhedral that surround and apparently replace earlier siderite. Other laminae consist entirely of very fine-grained ankerite. Textural relations are such that it cannot be determined if this ankerite is a primary precipitate or a secondary replacement mineral.

Microprobe analyses of ankerite (Fig. 20) in the slaty members are quite consistent around  $(\text{Ca}_{.52-.55}\text{Mg}_{.20}\text{Fe}_{.25-.26}\text{Mn}_{.01-.02})\text{CO}_3$ . It is considerably more iron rich in the Upper Cherty,  $(\text{Ca}_{.55}\text{Mg}_{.10}\text{Fe}_{.34}\text{Mn}_{.01})\text{CO}_3$ . Some ankerite from the Lower Cherty division contains appreciable manganese that substitutes for iron,  $(\text{Ca}_{.51}\text{Mg}_{.21}\text{Fe}_{.23}\text{Mn}_{.05})\text{CO}_3$ . As a general rule, samples that have abundant manganese in ankerite also have abundant manganese in siderite.

#### 4.4.3. *Kutnohorite-ferroan kutnohorite series*

Members of the kutnohorite-ferroan kutnohorite series  $[(\text{CaMn})(\text{CO}_3)_2\text{-Ca}(\text{Mn},\text{Mg},\text{Fe})(\text{CO}_3)_2]$  occur in the Lower Cherty division (Fig. 17). They have textural and paragenetic attributes broadly similar to those of the dolomite-ankerite series. However, the term dolomite is restricted to phases that have compositions normally close to pure  $\text{CaMg}(\text{CO}_3)_2$  with only small amounts of  $\text{Fe}^{+2}$  replacing Mg. In Drill Hole 1 there is continuous replacement of Mg by Fe through ankerite towards  $\text{CaFe}(\text{CO}_3)_2$ . Mn also replaces Mg in the dolomite structure, leading to the ideal kutnohorite composition  $[\text{CaMn}(\text{CO}_3)_2]$ . Inasmuch as the kutnohorite in Drill Hole 1 contain considerable iron  $[(\text{Ca}_{.48}\text{Mg}_{.19-.25}\text{Fe}_{.10-.15}\text{Mn}_{.12-.23})\text{CO}_3]$ , it is the ferroan variety.

#### 4.4.4. *Calcite*

Finally, crystalline euhedral grains of calcite  $[\text{CaCO}_3]$  are a major constituent in dolomitic limestone-bearing intervals at the top of the Biwabik Iron Formation. There it has a composition (Fig. 20) that deviates little from the ideal end-member composition  $[(\text{Ca}_{.98}\text{Mg}_{<.01}\text{Fe}_{.01}\text{Mn}_{<.01})\text{CO}_3]$ .

Calcite also occurs in slaty varieties of iron-formation in the uppermost part of the Upper Slaty division where it has an average composition  $(\text{Ca}_{.97}\text{Mg}_{.01}\text{Fe}_{.01}\text{Mn}_{.01})\text{CO}_3$ . Calcite is typically found in cherty varieties, as sparry pore cement that fills voids between silicate granules or within shrinkage cracks that transect silicate granules. It also occurs as mottles consisting of porphyroblasts that have included and replaced micritic chert-rich oolites, granules, and cement. In both varieties the composition of the calcite deviates little from  $(\text{Ca}_{.97}\text{Mg}_{.01}\text{Fe}_{.02}\text{Mn}_{.01})\text{CO}_3$ .

Subhedral grains of calcite also occur as interstitial cement in clastic strata interlayered within the basal red taconite toward the bottom of the iron-formation. That calcite is iron-rich and has an average composition  $(\text{Ca}_{.85}\text{Mg}_{.01}\text{Fe}_{.13}\text{Mn}_{.01})\text{CO}_3$ . Interstitial cement in the underlying Pokegama Quartzite contains appreciable manganese-rich calcite,  $(\text{Ca}_{.90}\text{Mg}_{.01}\text{Fe}_{.02}\text{Mn}_{.07})\text{CO}_3$ .

## 5. Zone 2: transitional iron-formation

Transitional iron-formation as defined by French (1968) contains mineral assemblages similar to those observed in unmetamorphosed iron-formation, but exhibits evidence of extensive recrystallization of quartz and magnetite and the widespread replacement of the iron silicates by quartz and ankerite. Such features include granules of very fine-grained acicular minnesotaite  $\pm$  trace amounts of micritic chert and magnetite that are typically fractured. The fractures are in turn filled with tabular grains of minnesotaite  $\pm$  quartz and  $\pm$  ankerite. Although these replacement features are quite pronounced, they in themselves are not necessarily related to emplacement of the Duluth Complex. Nonetheless, French (1968) placed the rocks of Zone 2 within the metamorphic aureole because of the partial reduction of hematite to magnetite in the lower red taconite and the appearance of clinozoisite in the underlying Pokegama Quartzite.

## 6. Zones 3 and 4: moderately and highly metamorphosed iron-formation

The boundary between Zone 2 and the moderately metamorphosed iron-formation of Zone 3 occurs about 2.3 miles from the contact with the Duluth Complex. It is marked by the appearance of a variety of amphibole phases and by the disappearance of original iron carbonates and silicates (Fig. 21). The development of grunerite-cummingtonite is pervasive throughout the zone and appears to have formed simultaneously in all rock types from both earlier iron silicates and iron carbonates.

Textual aspects similar to those in Zones 1 and 2 persist into Zone 3. However, the iron-formation throughout Zone 4 is completely recrystallized; most rock types are finely granular or hornfelsic. Some specific layers however, are locally medium to very coarsely-granular. These coarser-grained rocks are not foliated or lineated but have been described as granoblastic hornfels (Gundersen, 1960). Despite the considerable recrystallization, the original layered and laminated fabric is preserved and emphasizes the differences in the original bulk compositions.

### 6.1. Cummingtonite-grunerite series

Since the Reserve controversy of the 1970s, morphological attributes of the cummingtonite-grunerite series have attracted considerable attention, primarily because of their general resemblance to some asbestos-like minerals. However, to our knowledge, no detailed studies regarding specific stratigraphic, compositional, and structural attributes of these phases in the Biwabik Iron Formation have been completed. There is a general consensus, however, that these amphiboles formed under both prograde conditions, or as metamorphic temperatures increased and under retrograde conditions as temperatures decreased, in the metamorphic aureole.

The ideal end-member composition of cummingtonite is  $\text{Mg}_7\text{Si}_8\text{O}_{22}(\text{OH})_2$  and for grunerite it is  $\text{Fe}_7\text{Si}_8\text{O}_{22}(\text{OH})_2$ . However, French (1968), following the convention of Deer et al. (1963), subdivided the series using the ratio,  $R = \text{Fe}^{+2}/(\text{Fe}^{+2} + \text{Fe}^{+3} + \text{Mn} + \text{Mg})$ . In that scheme, amphiboles with an R-value of greater than 0.7 are termed grunerite. The term cummingtonite is applied to those with a more magnesium-rich ratio. Despite the data having considerable scatter, French (1968) concluded that there is a general increase in Mg content with proximity of the Duluth Complex (Fig. 22). Values of R less than 0.7 (or cummingtonite) typically appear within one mile of the contact. French however, did not give enough textural information to determine which of the amphiboles he analyzed were prograde or retrograde. Nonetheless, these data agree with the observations of Gundersen and Schwartz (1962) who identified prograde cummingtonite

near the gabbro, and those of Morey and others (1972) who established the presence of prograde grunerite well away from the gabbro.

Prograde grunerite first occurs in Zone 3 as small, tabular crystals surrounded by radiating fibrous sheaves composed of fine needles (Fig. 23). Prograde grunerite in Zone 4 forms well developed acicular grains (Fig. 24), which gave way to the east to medium-size prismatic grains that are colorless and display evidence of well developed polysynthetic twinning (Gundersen and Schwartz, 1962).

Still farther to the east and immediately adjacent to the Duluth Complex, paragenetic relationships are complicated by the presence of retrograde cummingtonite that is medium to coarse grained and prismatic. For example, virtually all of the prismatic cummingtonite at the Dunka River locality appears to be paragenetically late, having formed partly from fayalite, but mainly from ferrosilite/pigeonite (Bonnichsen, 1969). At somewhat lower temperatures, prismatic cummingtonite may be replaced by more magnesium-rich phases that have an acicular habit. At still lower temperatures prograde acicular grunerite may be replaced by acicular or fibrous cummingtonite. Many of these retrograde reactions seem to involve the development of secondary magnetite (Gunderson and Schwartz, 1960).

## 6.2. Other silicates

Zones 3 and 4 also contain a variety of other iron silicates. The clinopyroxene, hedenbergite, first appears as a prograde phase in the metamorphic aureole about 1.7 miles from the contact with the Duluth Complex. It defines the outer fringe of Zone 4. Other mineralogic changes that occur as the contact with the Duluth Complex is approached include the disappearance of hematite and its replacement by magnetite and the appearance of fayalite, and immediately adjacent to the contact, ferrosilite.

Fayalite is restricted to cherty divisions within Zone 4. Typically, it occurs as small anhedral grains that contain included grains of older-formed minerals (Fig. 25). The origin of the fayalite is somewhat equivocal. Textural features imply that it formed by a reaction involving quartz and magnetite (Gundersen and Schwartz, 1962). Other textural evidence implies that it evolved from siderite like that seen in Zone 1 (Morey et al., 1972) or by a reaction involving quartz and grunerite as in Zone 2 (French, 1968). Regardless of textural attributes, the fayalite occurs over a very restricted iron-rich compositional range.

A calcium pyroxene, hedenbergite, is abundant throughout the iron-formation in Zones 3 and 4. It is medium to coarse-grained and generally forms interlocking aggregates, layers, or mottles. Analyzed grains from Zone 3 display a wide range of compositions marked by substitution of magnesium for iron (Morey et al., 1970). Textural evidence implies that hedenbergite takes the place of the ankerite found in unmetamorphosed iron-formation (Morey et al., 1970). The amphibole hornblende occurs as both prograde and retrograde phases. Prograde hornblende occurs intergrown with hedenbergite in the lower part of Zone 4 (Fig. 26). More commonly however, very fine acicular to fibrous hornblende is a retrograde phase that replaces hedenbergite, mainly at grain margins. Retrograde, acicular grunerite is also commonly found surrounding grains of hedenbergite (Fig. 27).

Phases of the enstatite-ferrosilite series (Deer et al., 1992) originally identified as ferrohypersthene (Gundersen and Schwartz, 1962; Bonnichsen, 1975) are widespread and abundant throughout Zone 4; they are the most abundant silicate at the Dunka River locality (Bonnichsen, 1975) at the far eastern end of the range. It occurs primarily as large, tabular

crystals that in part initially crystallized as pigeonite and then inverted to ferrosilite during cooling. As previously noted it has been extensively replaced by cummingtonite.

Two garnet varieties were identified in Zone 4 of the Biwabik Iron Formation, almandine ( $\text{Fe}_3\text{Al}_2\text{Si}_3\text{O}_{12}$ ) and andradite ( $\text{Ca}_3\text{Fe}_2\text{Si}_3\text{O}_{12}$ ). The almandine is more abundant and is found to be present in the lower part of the Lower Slaty division and the lower part of the Lower Cherty division (Morey et al., 1972). The garnet occurs as euhedral grain typically with cores of earlier minerals (Fig. 28).

## 7. Conclusions

Textures and mineral compositions associated with both unmetamorphosed and metamorphosed Biwabik Iron Formation are complex. The iron-formation is heterogeneous on a scale of a few inches to a few feet. Thus, any single mineral or mineral assemblage is a function of the bulk composition of the specific bed involved. At the east end of the range, further complexities arise from superimposed metamorphic conditions associated with the emplacement of the Duluth Complex. New minerals formed both under prograde conditions as metamorphic temperatures increased and under retrograde conditions as temperatures decreased. Therefore, one cannot assume that the mineralogy in one mine or part of the Range will be identical in correlative units in other mines or parts of the Range.

## 8. Acknowledgments

The Minnesota Legislator as administrated by the Minnesota Minerals Coordinating Committee provided funding for much of this study, while the Minnesota Geological Survey employed the authors.

## References

- Bonnichsen, B., 1969. Metamorphic pyroxenes and amphiboles in the Biwabik Iron Formation, Dunka River area, Minnesota, *in* Pyroxenes and amphiboles: Crystal chemistry and phase petrology. Mineralogical Society of America Special Paper 2, 217-239.
- Bonnichsen, B., 1975. Geology of the Biwabik Iron Formation, Dunka River area, Minnesota. *Economic Geology* 70, 319-340.
- Deer, W.A., Howie, R.A., and Zussman, J., 1963. *Rock-Forming Minerals* (5 vols.). Wiley, New York.
- Deer, W.A., Howie, R.A., and Zussman, J., 1992. *An introduction to rock-forming minerals*, 2<sup>nd</sup> Edition. Prentice Hall, London, 696 p.
- French, B.M., 1968. Progressive contact metamorphism of the Biwabik Iron-formation, Mesabi Range, Minnesota. *Minnesota Geological Survey Bulletin* 45, 103 p.

- French, B.M., 1973. Mineral assemblages in diagenetic and low-grade metamorphic iron-formation, in Precambrian iron-formations of the world. *Economic Geology* 68 (7), 1063-1074.
- Griffin, W.L., and Morey, G.B., 1969. The geology of the Isaac Lake quadrangle, St. Louis County, Minnesota. Minnesota Geological Survey Special Publication Series SP-8, 57 p.
- Gruner, J.W., 1936. The structure and composition of greenalite. *American Mineralogist* 21, 449-455.
- Gruner, J.W., 1944. The composition and structure of minnesotaite, a common iron silicate in iron formation. *American Mineralogist* 29, 363-372.
- Gruner, J.W., 1946. The mineralogy and geology of the taconites and iron ores of the Mesabi range, Minnesota. St. Paul, Office of the Commissioner of the Iron Range Resources and Rehabilitation, 127 p.
- Gundersen, J.N., 1960. Stratigraphy of the eastern Mesabi district, Minnesota. *Economic Geology* 55, 1004-1029.
- Gundersen, J.N., and Schwartz, G.M., 1962. The geology of the metamorphosed Biwabik Iron-Formation, Eastern Mesabi district, Minnesota. Minnesota Geological Survey Bulletin 43, 139 p.
- Jirsa, M.A., Miller, J.D.Jr., and Morey, G.B., 2004. Geology of the Biwabik Iron Formation and Duluth Complex, this volume.
- Klein, Jr., C., 1974. Greenalite, stilpnomelane, minnesotaite, crocidolite and carbonates in a very low-grade metamorphic Precambrian iron-formation. *Canadian Mineralogist* 12, 475-498.
- Klein, Jr., C., 1983. Diagenesis and metamorphism of Precambrian banded iron-formations, in Trendall A.S. and Morris, R.C., eds, *Iron-Formations. Facts and Problems*, New York, Elsevier, 417-469.
- LaBerge, G.L., 1967. Microfossils and Precambrian iron-formations. *Geological Society of America Bulletin* 78 (3), 331-342.
- Mengel, J.T. Jr., 1965. Precambrian taconite iron formation: A special type of sandstone. Geological Society of America, 79<sup>th</sup> Annual Meeting, Kansas City, Missouri, 1965, Program, p. 106.
- Miyano, T., 1987. Diagenetic to low grade metamorphic conditions of Precambrian iron-formation, in: Uipterdijk Apple, P.W., and LaBerge, G.L., (Eds.), *Precambrian Iron-Formations*. Theophrastus Publications, Athens, pp.155-186.

Morey, G.B., 2003. Paleoproterozoic Animiekie Group related rocks and associated iron ore deposits in the Virginia Horn, *in* Jirsa, M.A., and Morey, G.B., eds, Contributions to the Geology of the Virginia Horn Area, St. Louis County, Minnesota. Minnesota Geological Survey Report of Investigation 53, 74-102.

Morey, G.B., Papike, J.J., Smith, R.W., and Weiblen, P.W., 1972. Observations on the contact metamorphism of the Biwabik Iron-formation, east Mesabi district, Minnesota, *in* Doe, B.R., and Smith, D.K., eds., Studies in mineralogy and Precambrian geology. Geological Society of America Memoir 135, 225-264.

Wolff, J.F., 1917. Recent geologic developments on the Mesabi Iron Range, Minnesota. American Institute of Mining and Metallurgical Engineers, Transactions 56, 229-257.

### Figure Captions

Figure 1: Simplified geologic map and stratigraphic section of the Mesabi Iron Range. The main geologic unit is the Biwabik Iron Formation (shown in gray). The stratigraphic section shows the lateral distribution of the units of the iron formation, the Upper Slaty, Upper Cherty, Lower Slaty, and Lower Cherty (after Jirsa et al., (this volume))

Figure 2: Stratigraphic section and mineralogy of the E.J Longyear Drill Hole #1. It was drilled as a long stratigraphic test hole and was finished in 1910. Its location is shown in Figure 1.

Figure 3: Compositional relationships between the main silicate minerals of Zone 1 in the Biwabik Iron-Formation.

Figure 4: Optical image of chamosite granules in a quartz matrix. Field of view is 900 microns across.

Figure 5: Relationships between the ideal compositions of chamosite, clinochlore, greenalite, and serpentine (antigorite).

Figure 6: Variations in the compositions of clinochlore (chlorite), chamosite and greenalite as a function of stratigraphic division.

Figure 7: Optical image of a greenalite granule surrounded by minnesotaite matrix. Field of view is 900 microns across.

Figure 8: Backscattered electron image of a greenalite granule surrounded by minnesotaite matrix. Field of view is about 240 microns across.

Figure 9: Optical image of a minnesotaite granule in minnesotaite matrix. The granule exhibits shrinkage cracks. Field of view is 400 microns across.

Figure 10: Compositional plot of minnesotaite and talc as a function of depth.

Figure 11: Optical image showing granules of chamosite (on the left) and stilpnomelane (on the right). Field of view is 1800 microns across.

Figure 12: Optical image of stilpnomelane blades in a quartz matrix. Field of view is 600 microns across.

Figure 13: Backscattered electron image of stilpnomelane needles in a carbonate matrix.

Figure 14: Optical image of siderite with a stilpnomelane core. Field of view is 500 microns across.

Figure 15: Compositional plots of stilpnomelane and chamosite.

Figure 16: Compositional relationships within the carbonate system  $\text{CaCO}_3\text{-MgCO}_3\text{-MnCO}_3\text{-FeCO}_3$

Figure 17: Manganese-content as a function of depth of the carbonates in the Biwabik Iron Formation

Figure 18: Backscattered electron image of a zoned ankerite crystal. The dark bands are richer in magnesium and the lighter bands are richer in iron.

Figure 19: Optical image of an ankerite granule surrounded by later ankerite growth. Granule is about 600 microns in diameter.

Figure 20: Compositional plots of the carbonates in the Biwabik Iron Formation.

Figure 21: Mineral occurrences in the Biwabik Iron Formation as a function of distance from the contact with the Duluth Complex.

Figure 22: Composition of cummingtonite-grunerite in the Biwabik Iron Formation relative to distance from the Duluth Complex.

Figure 23: Optical image of fibrous grunerite in a matrix of quartz from the metamorphic contact zone with the Duluth Complex. Field of view is about 1000 microns across.

Figure 24: Optical image of acicular grunerite in a matrix of quartz from Zone 4. Field of view is about 1000 microns across.

Figure 25: Optical image of fayalite (Fay) intergrown with hornblende (Hornb) and carbonate (Carb). Field of view is about 600 microns across.

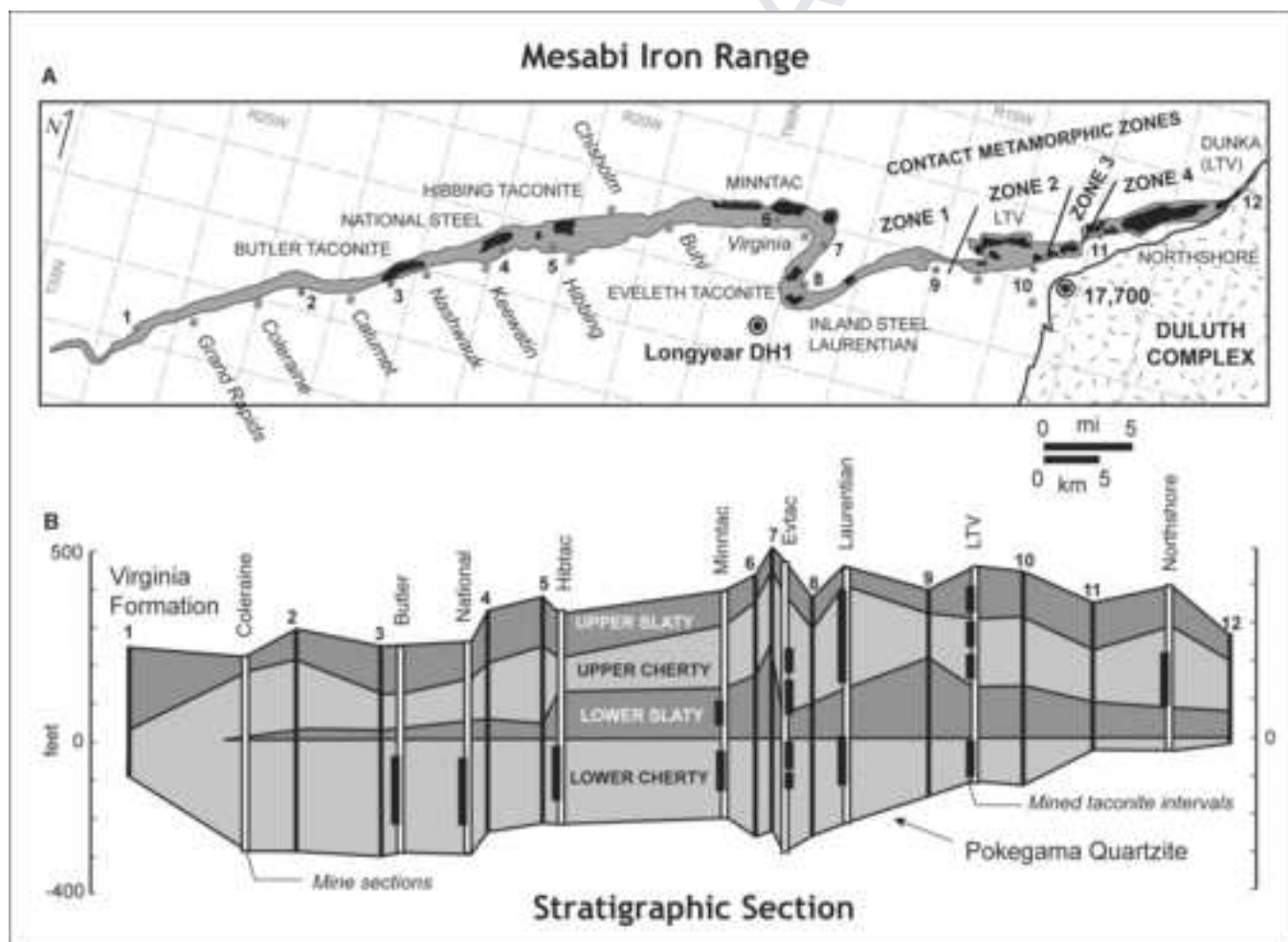
Figure 26: Optical image of hornblende (Hornb) and hedenbergite (Hedenb) from Zone 4. Field

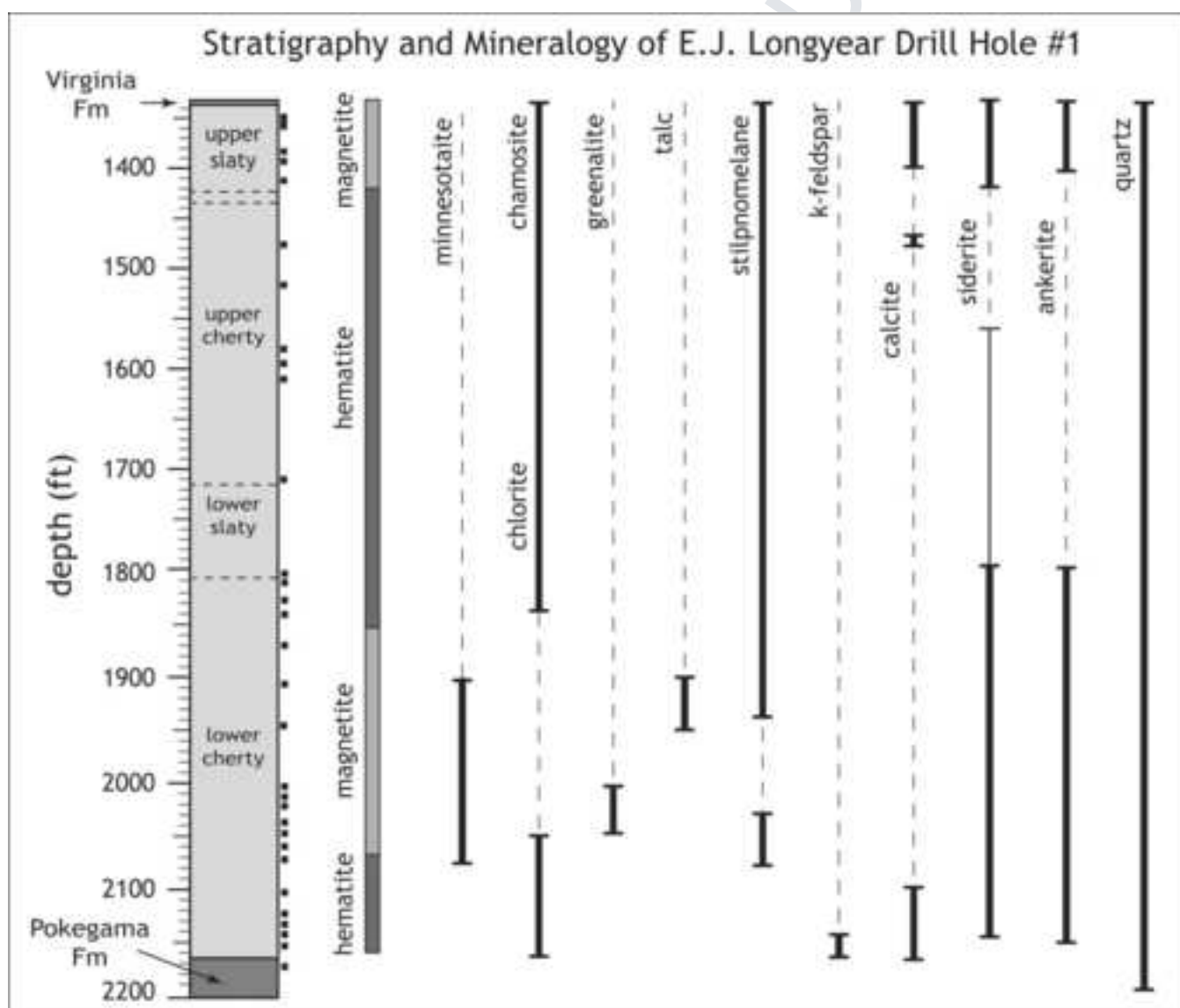
of view is about 1000 microns across.

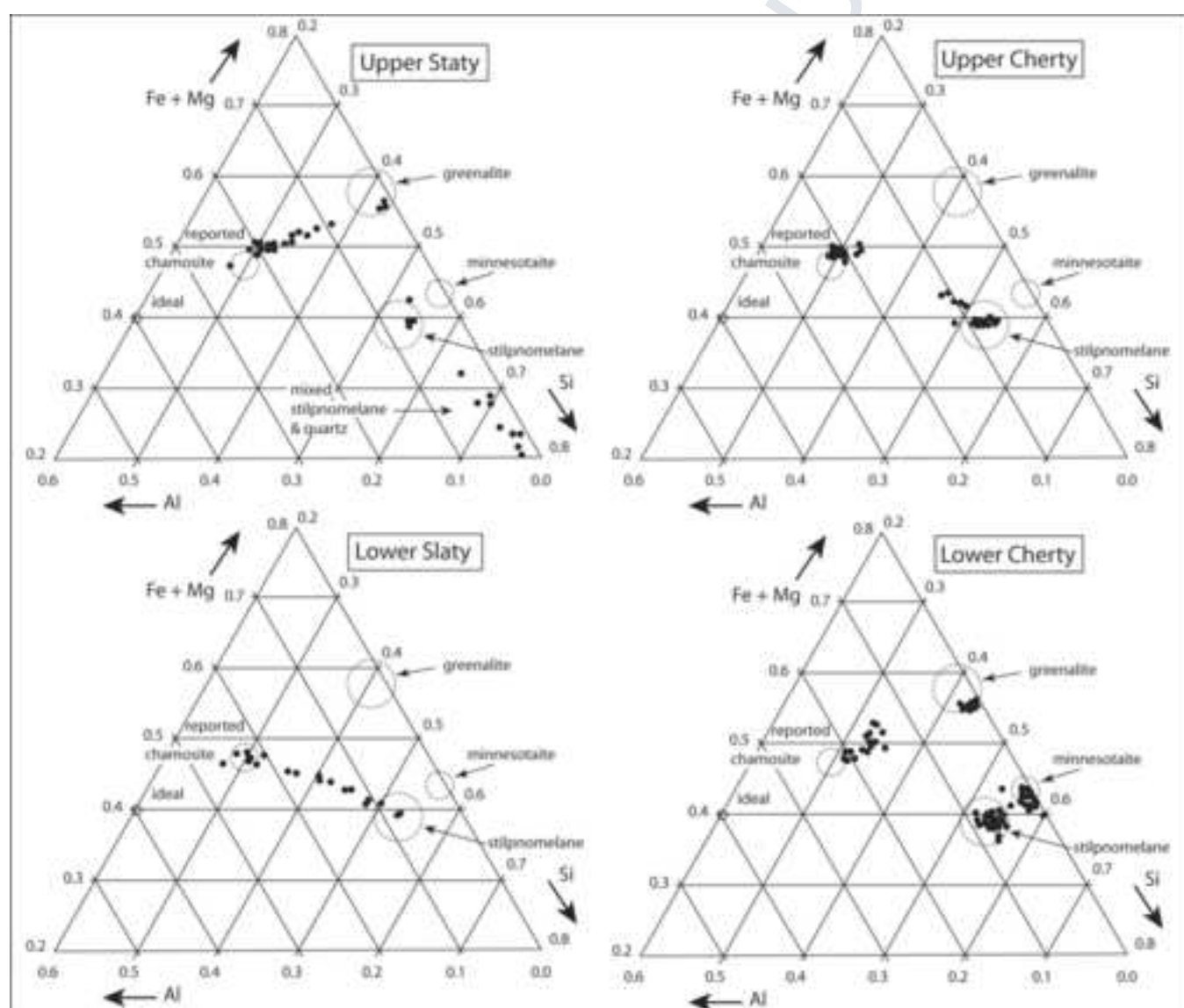
Figure 27: Optical image of retrograde grunerite surrounding hedenbergite. Field of view is about 550 microns across.

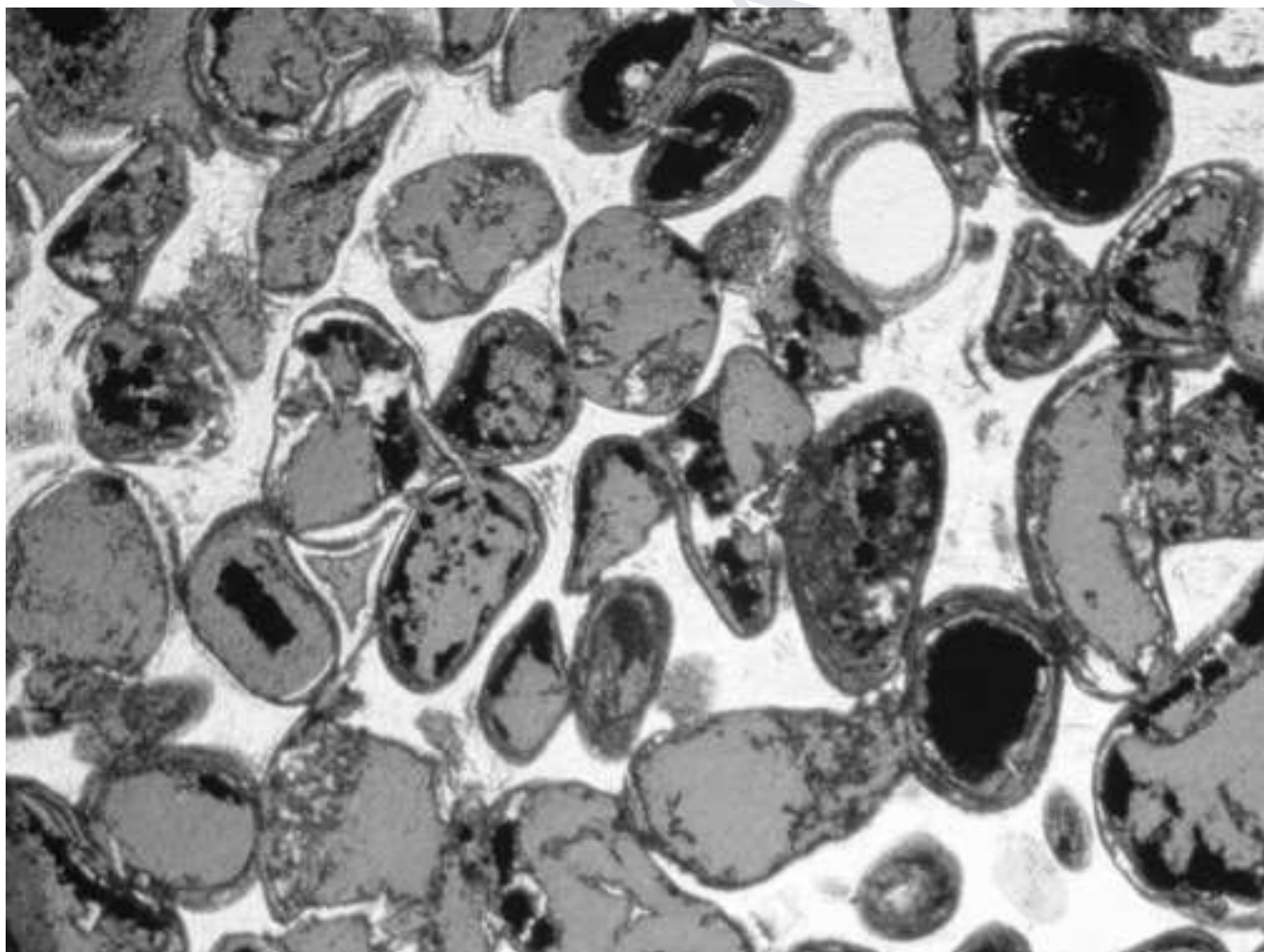
Figure 28: Optical image of almandine garnet in a matrix of grunerite, magnetite and carbonaceous materials. Field of view is about 600 microns across.

MANUSCRIPT

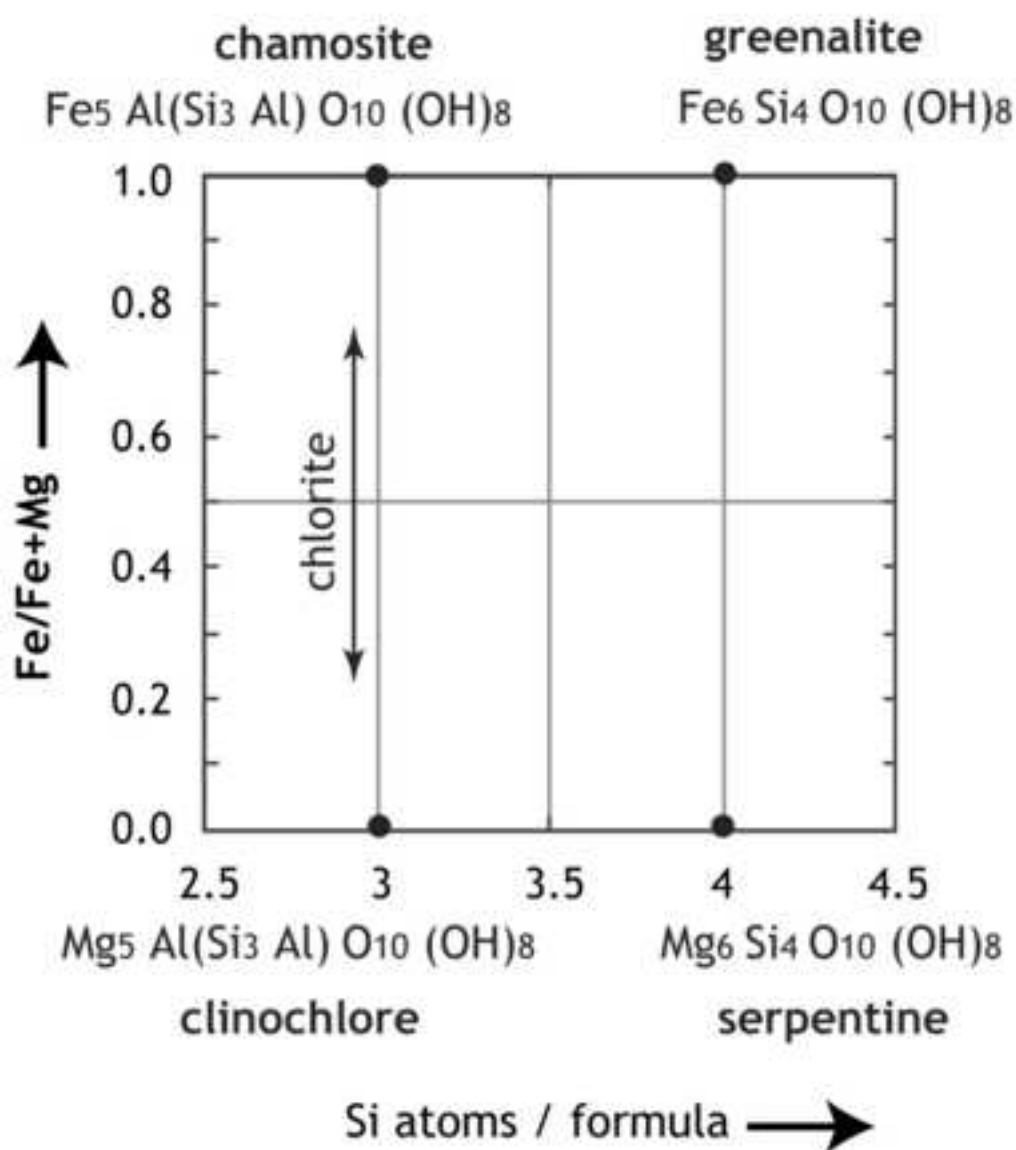


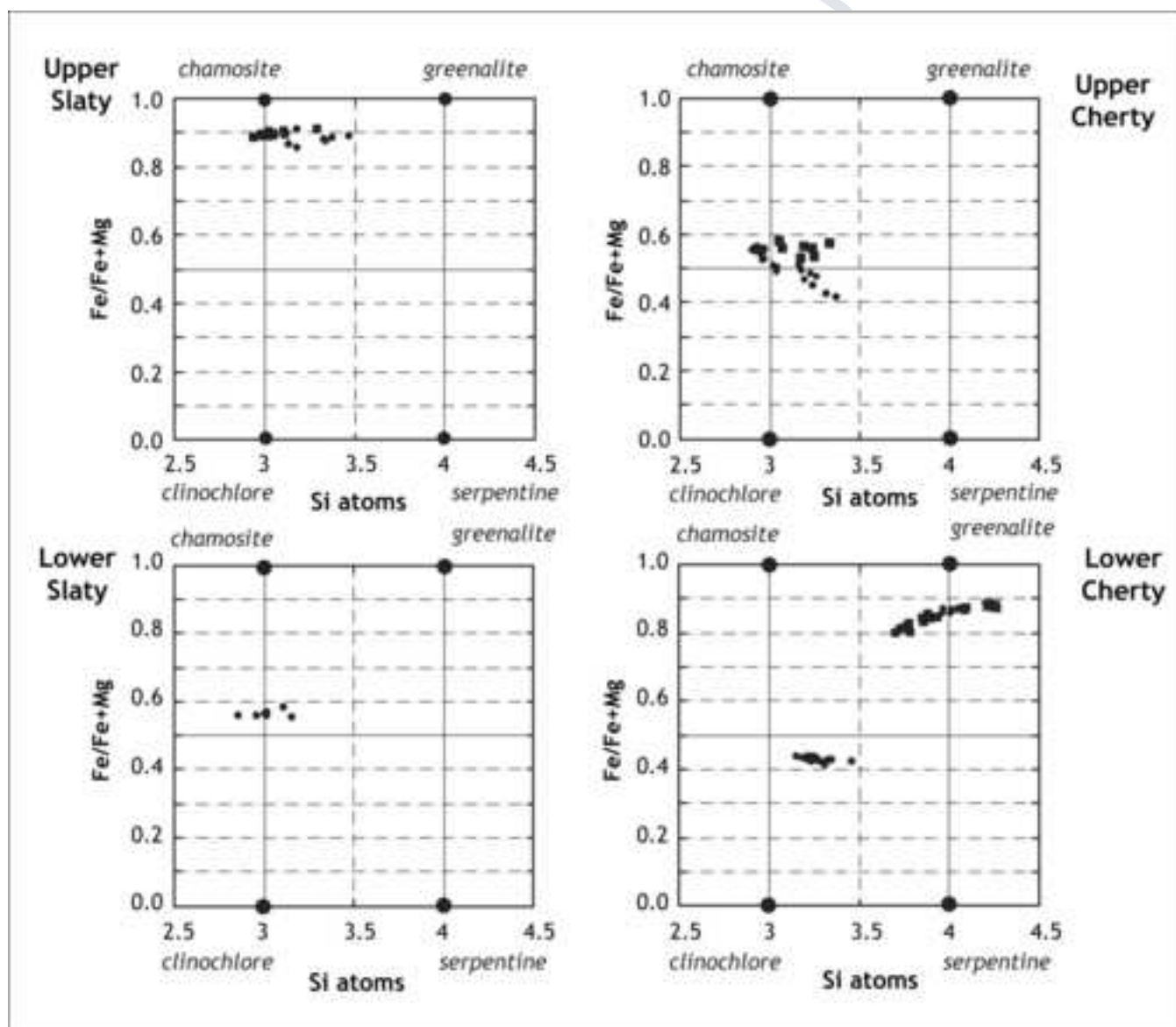


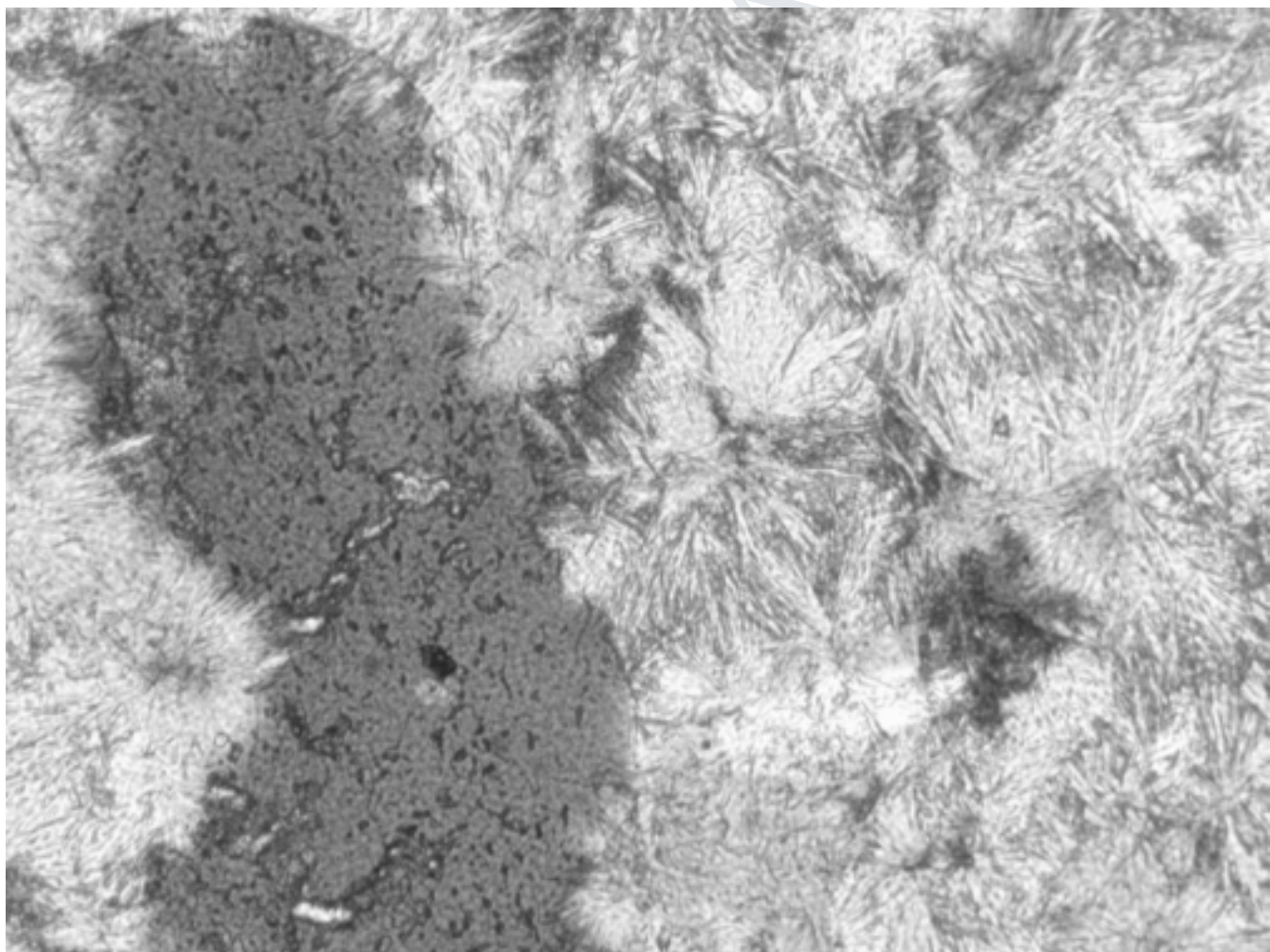


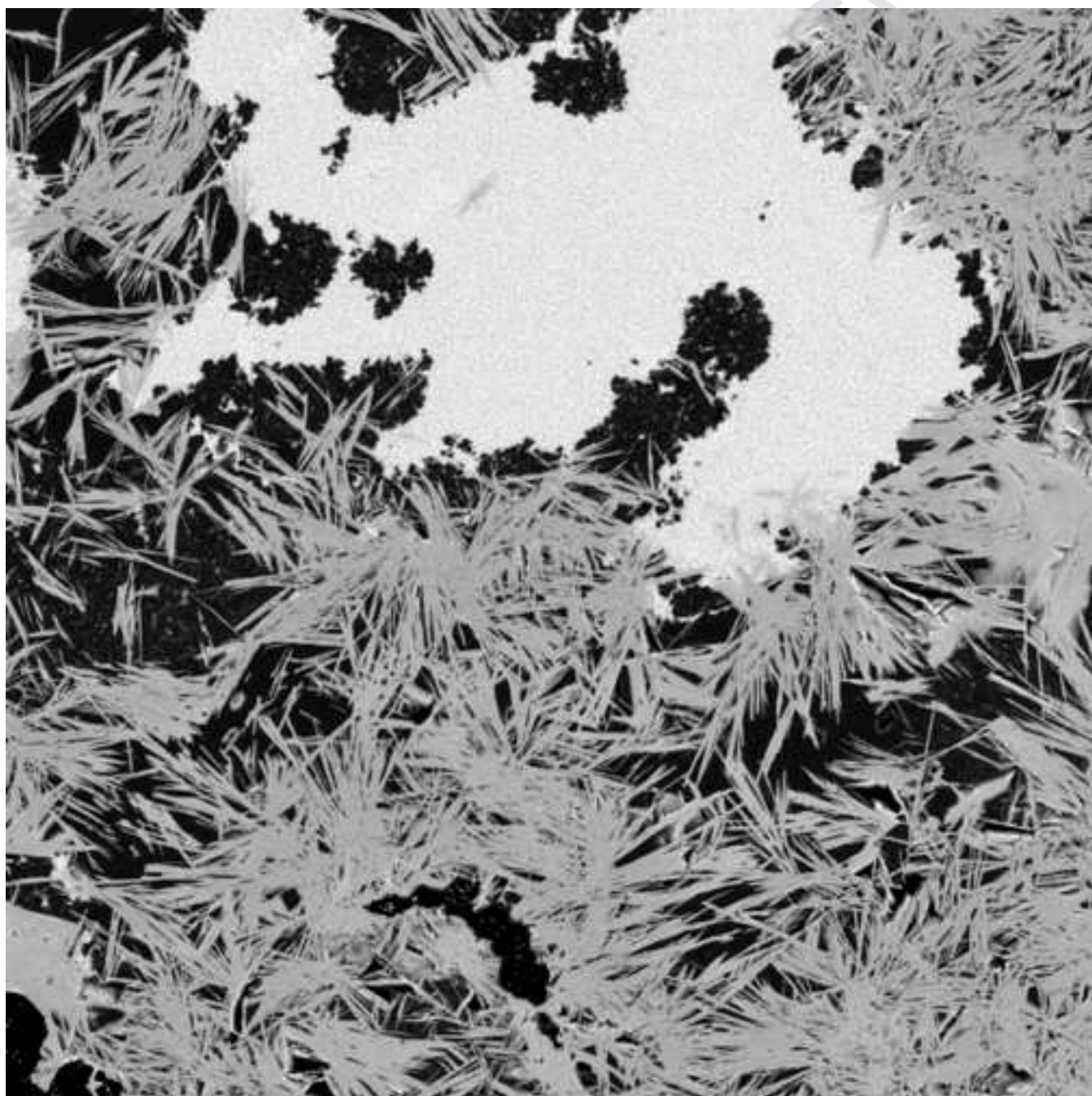


# Compositional Relationships Between Chamosite, Clinochlore, Greenalite and Serpentine

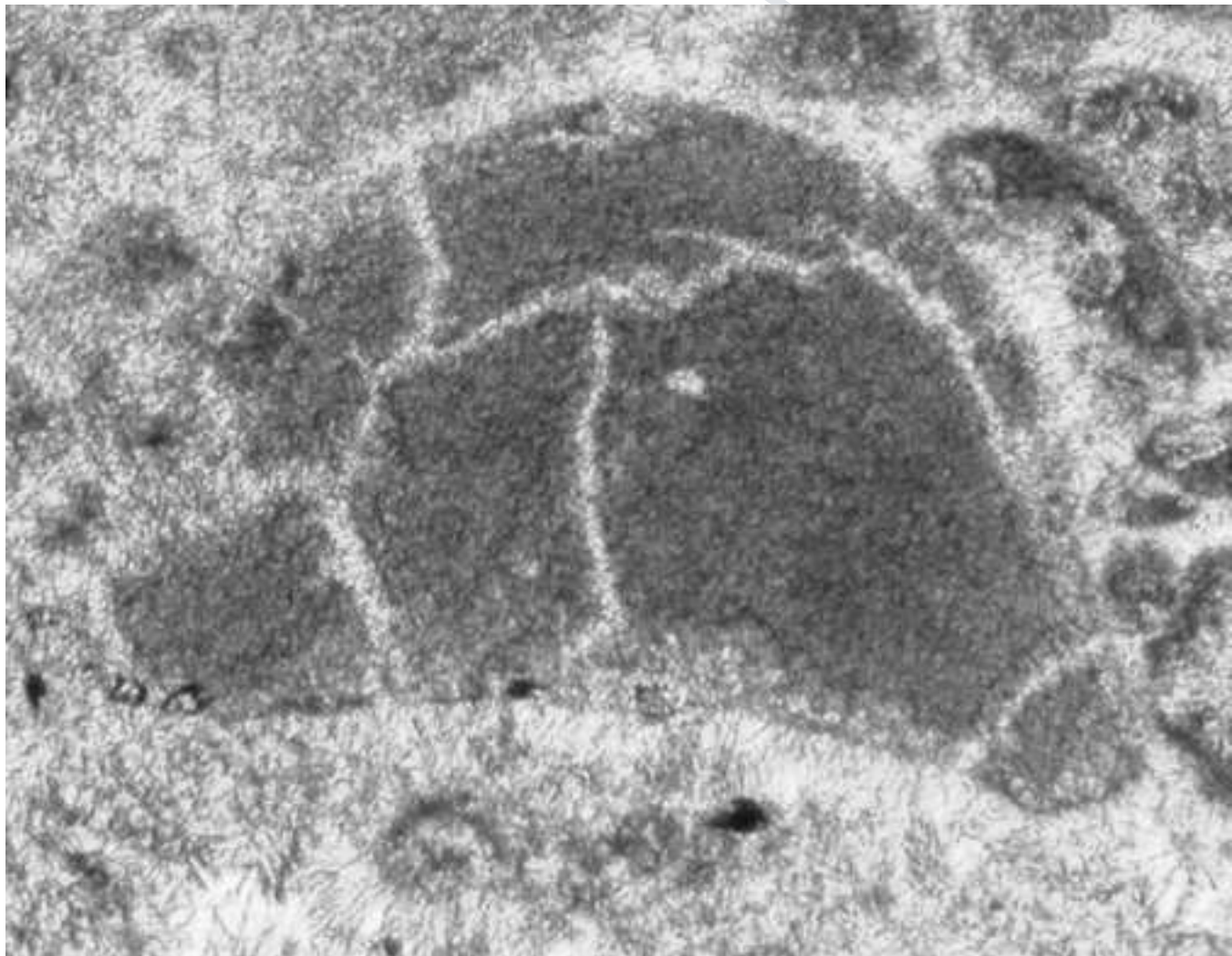


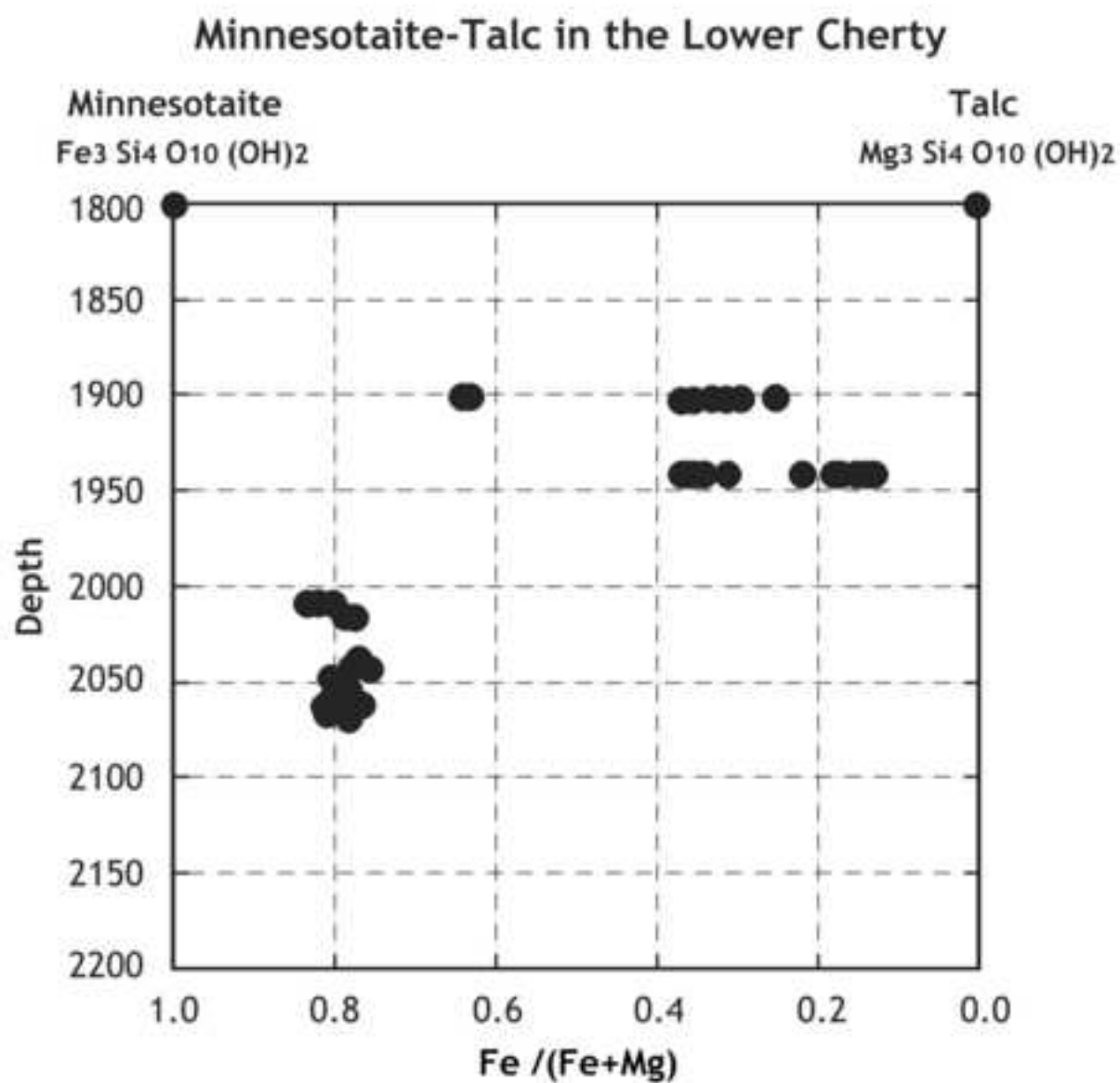


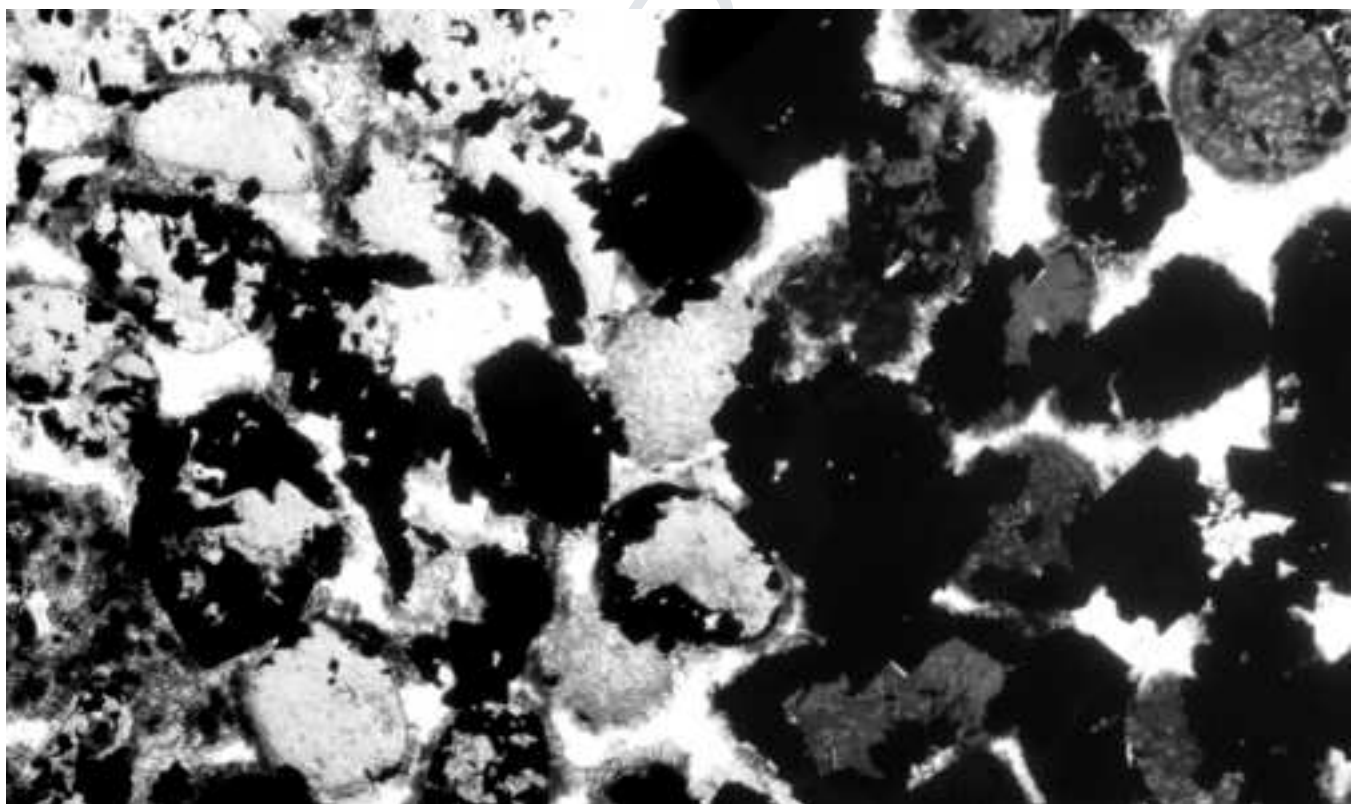




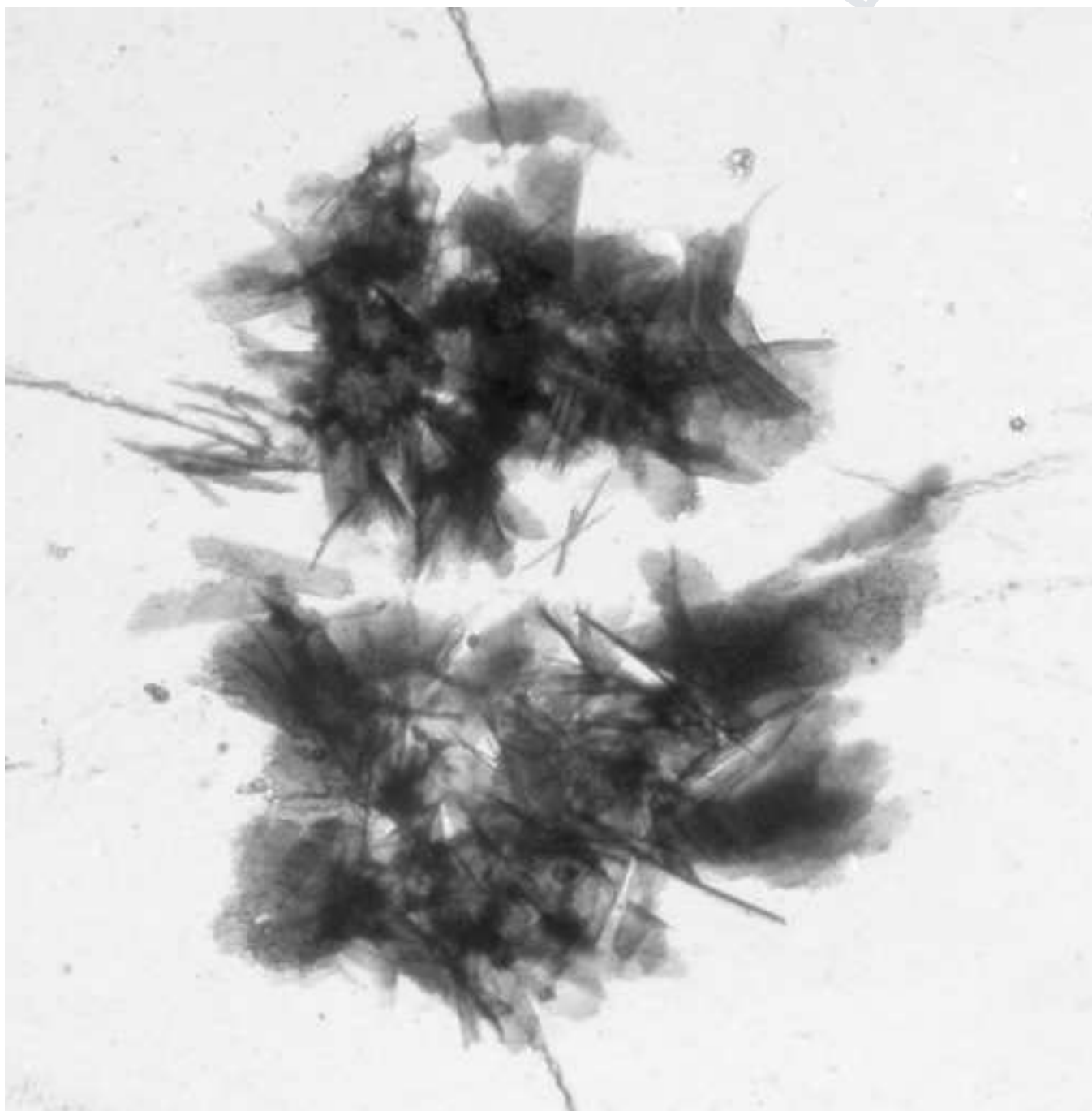
MANUSCRIPT

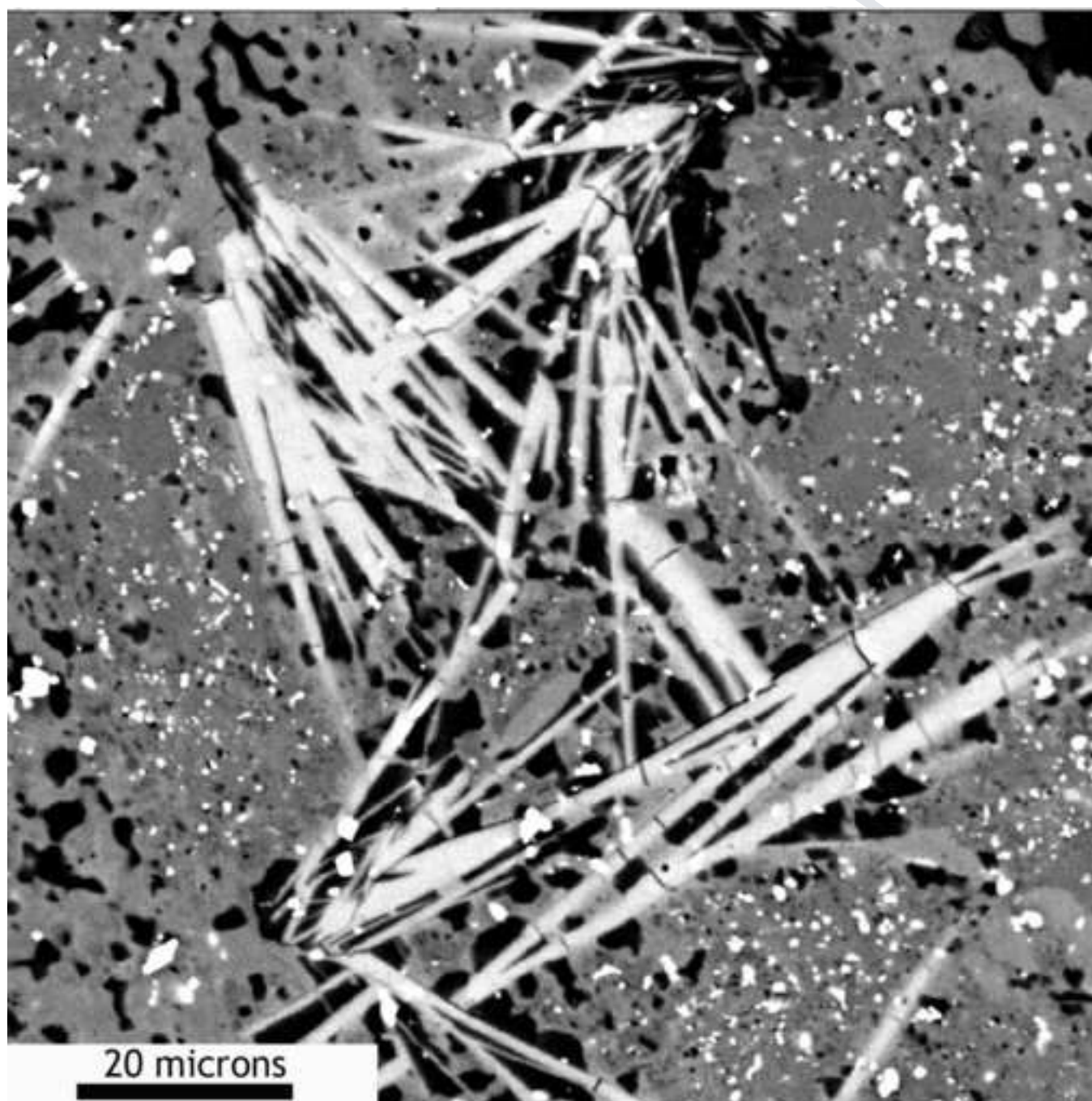


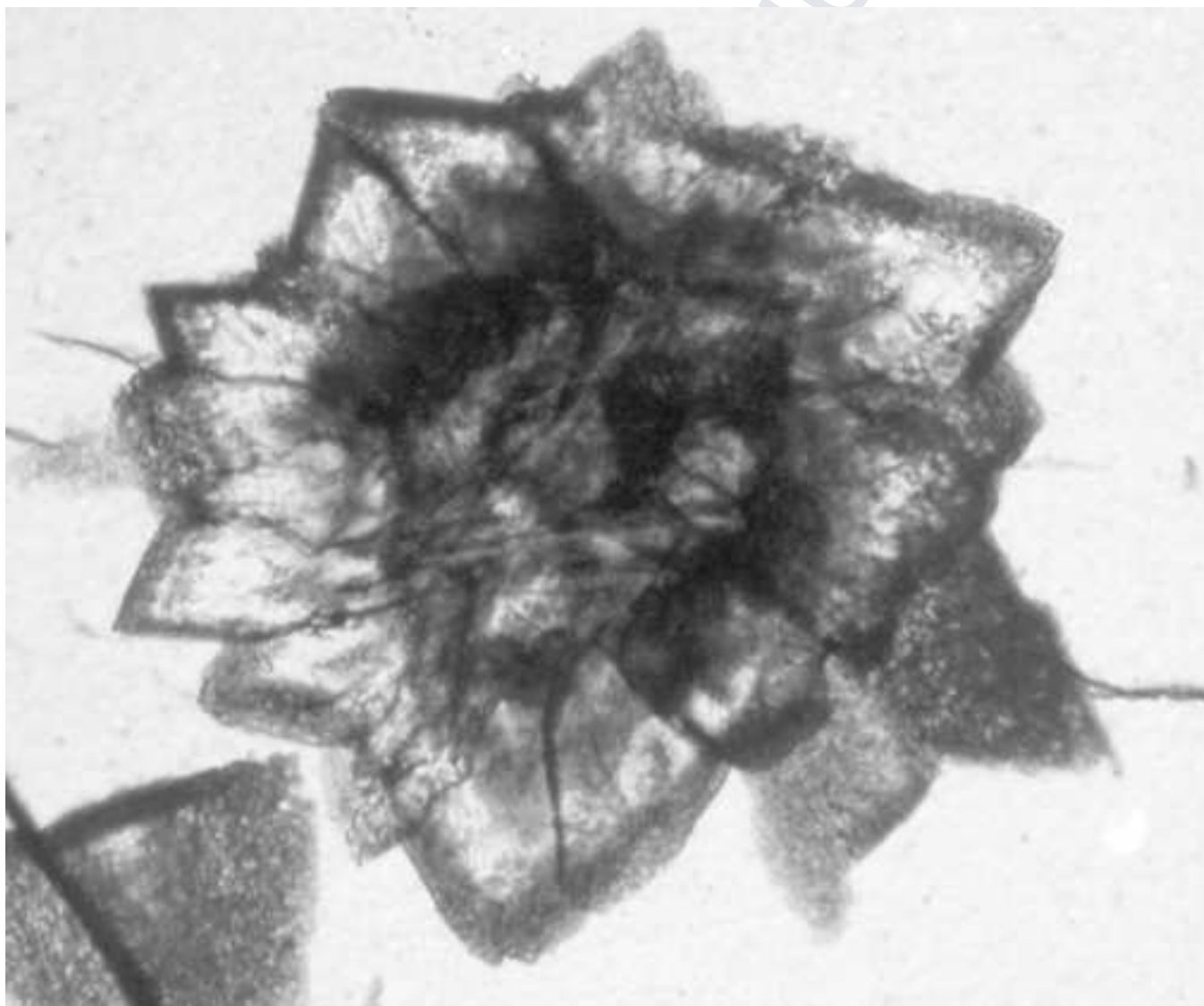


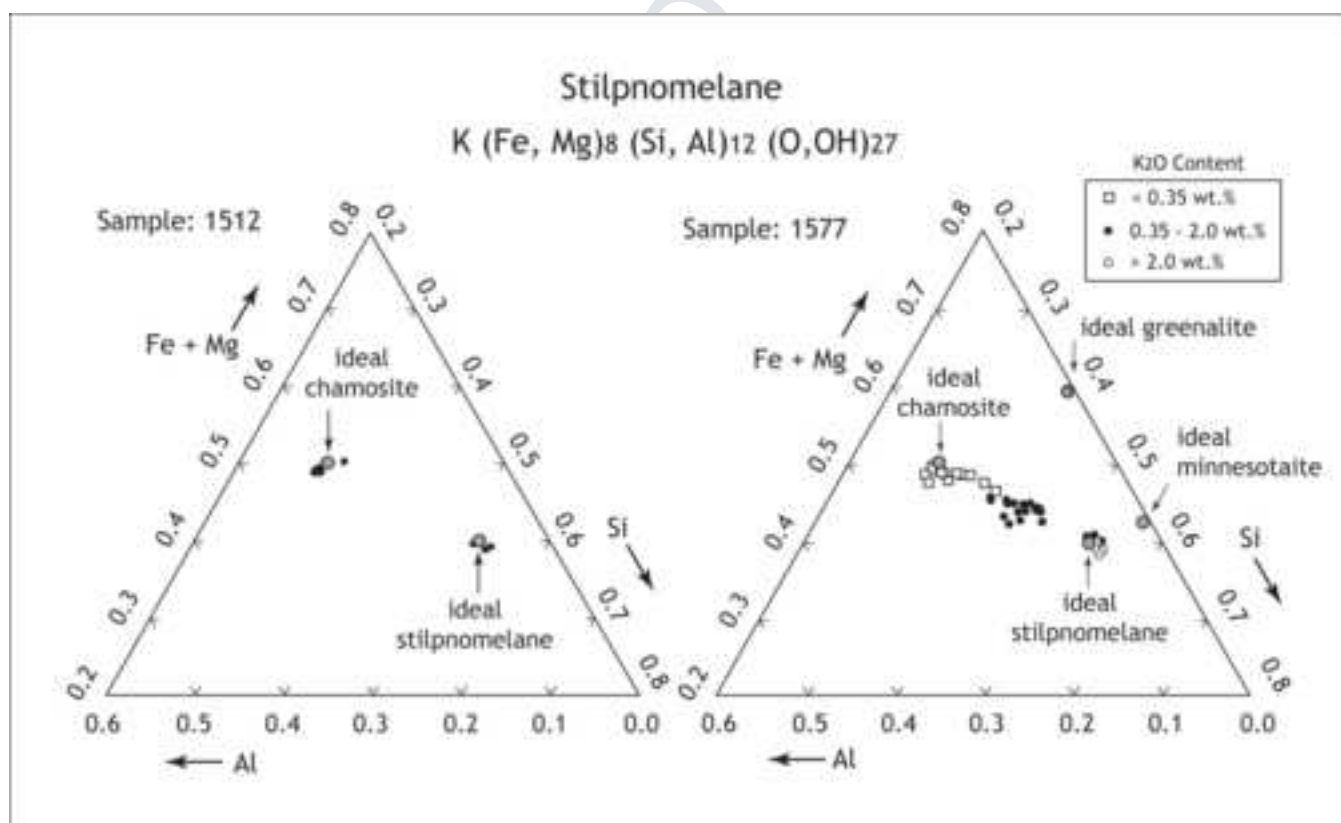


RIPT

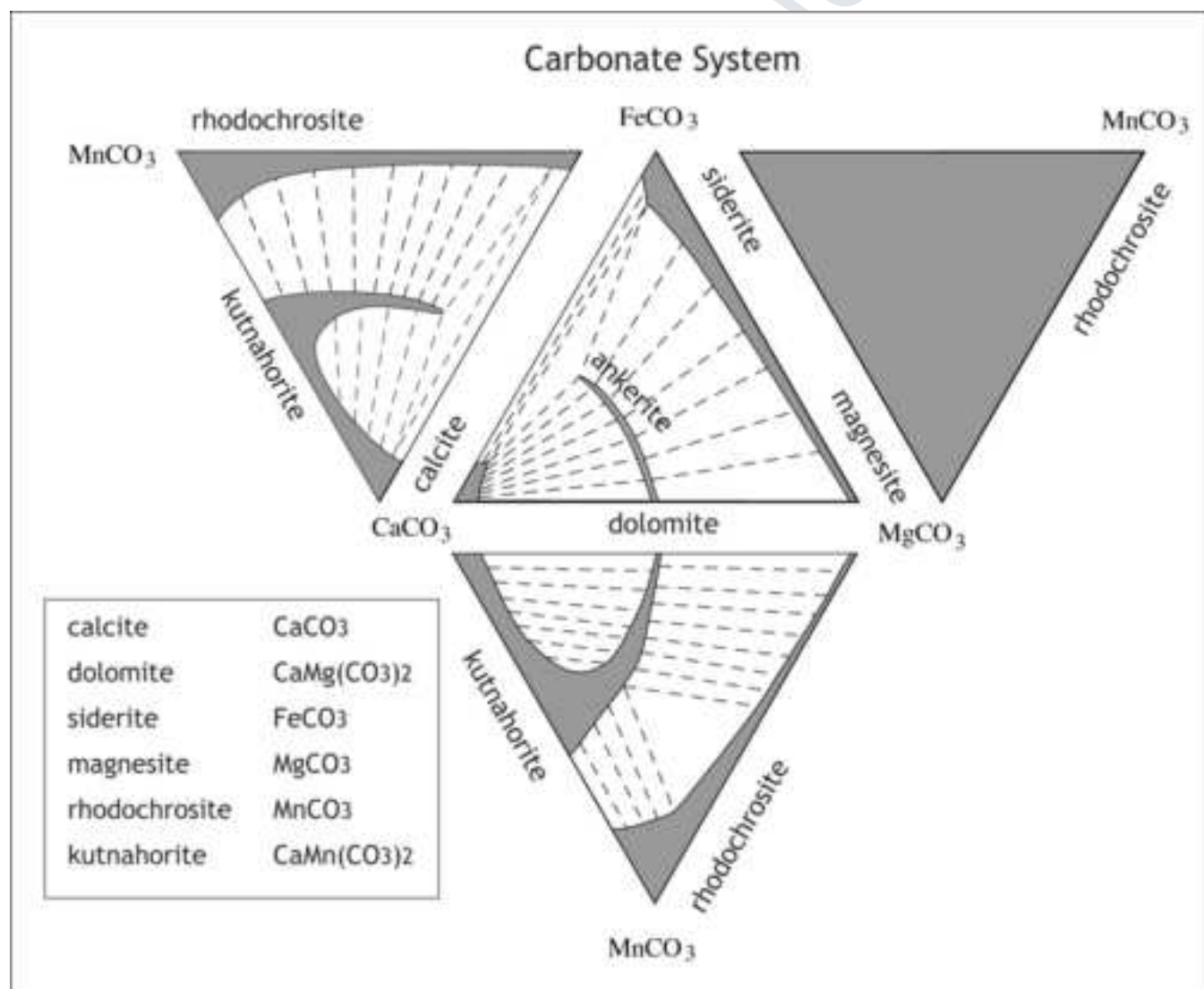


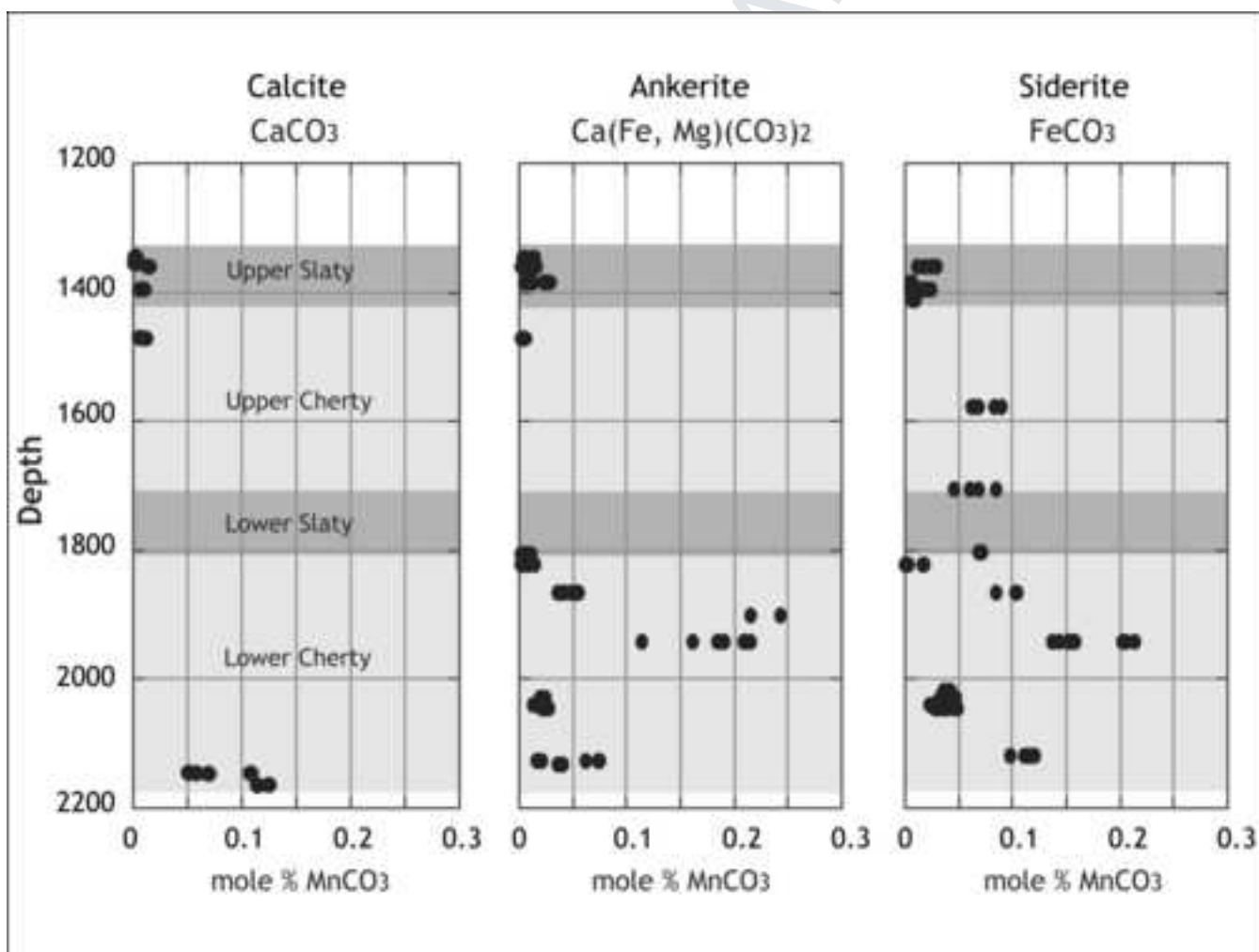


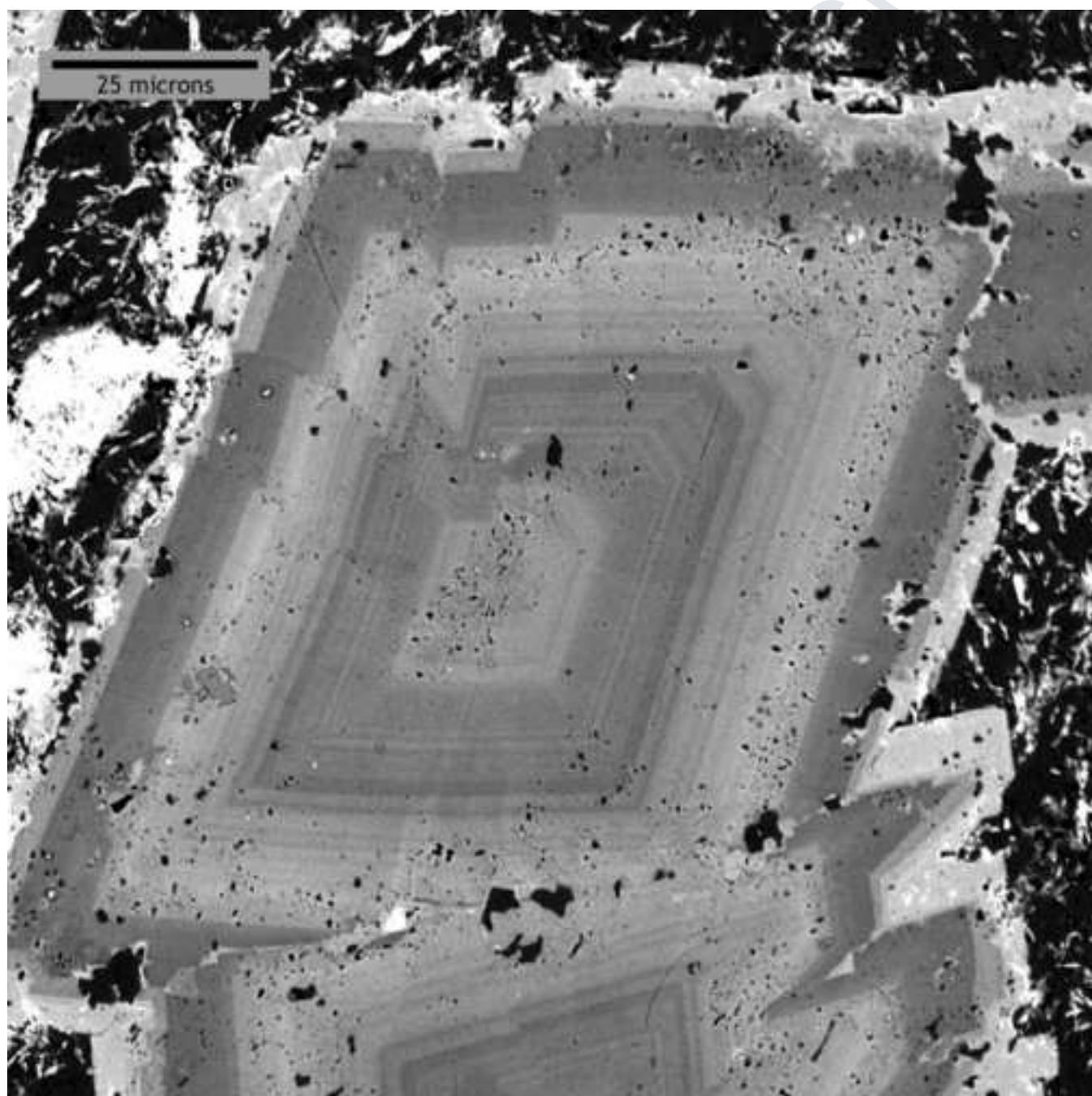


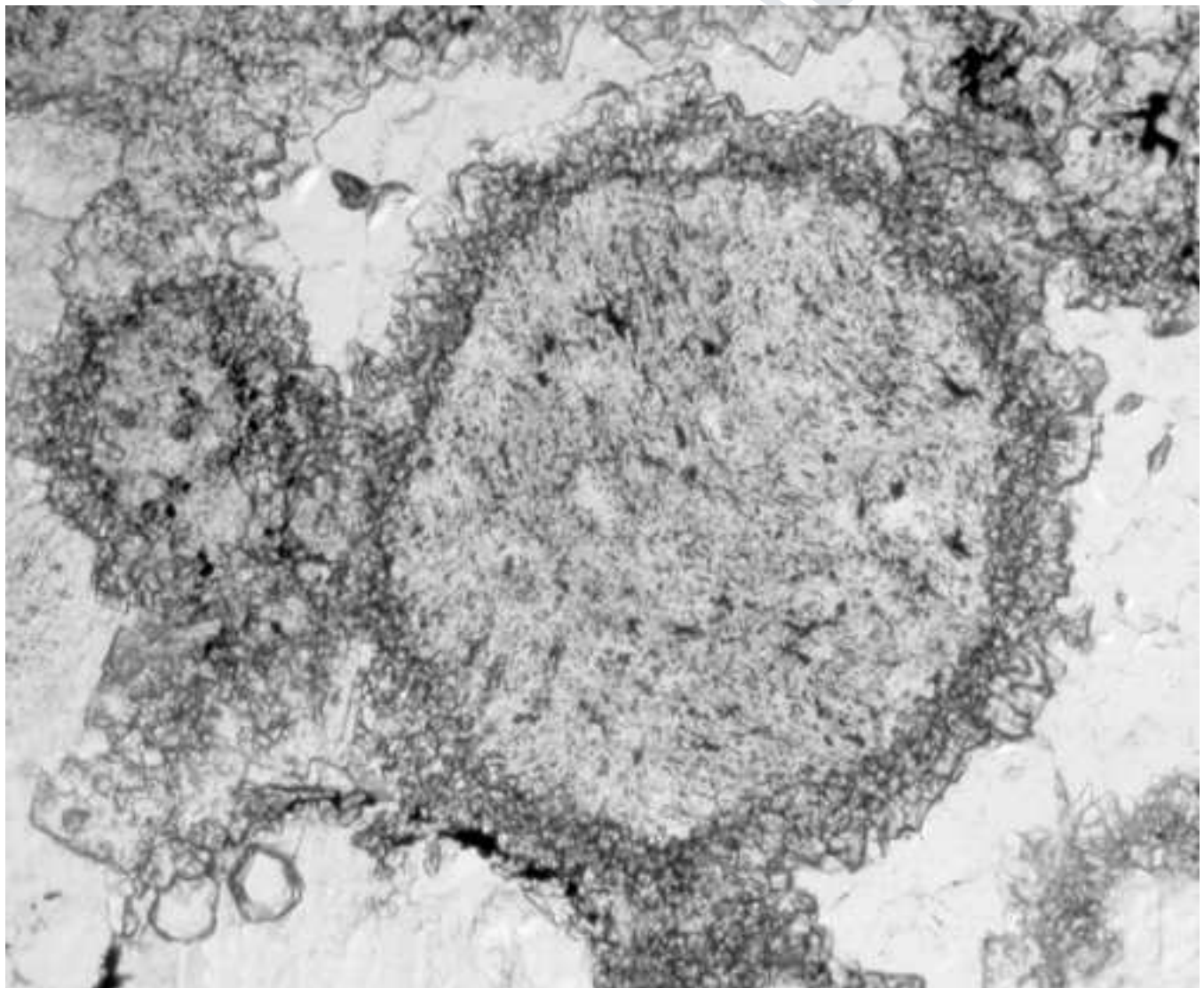


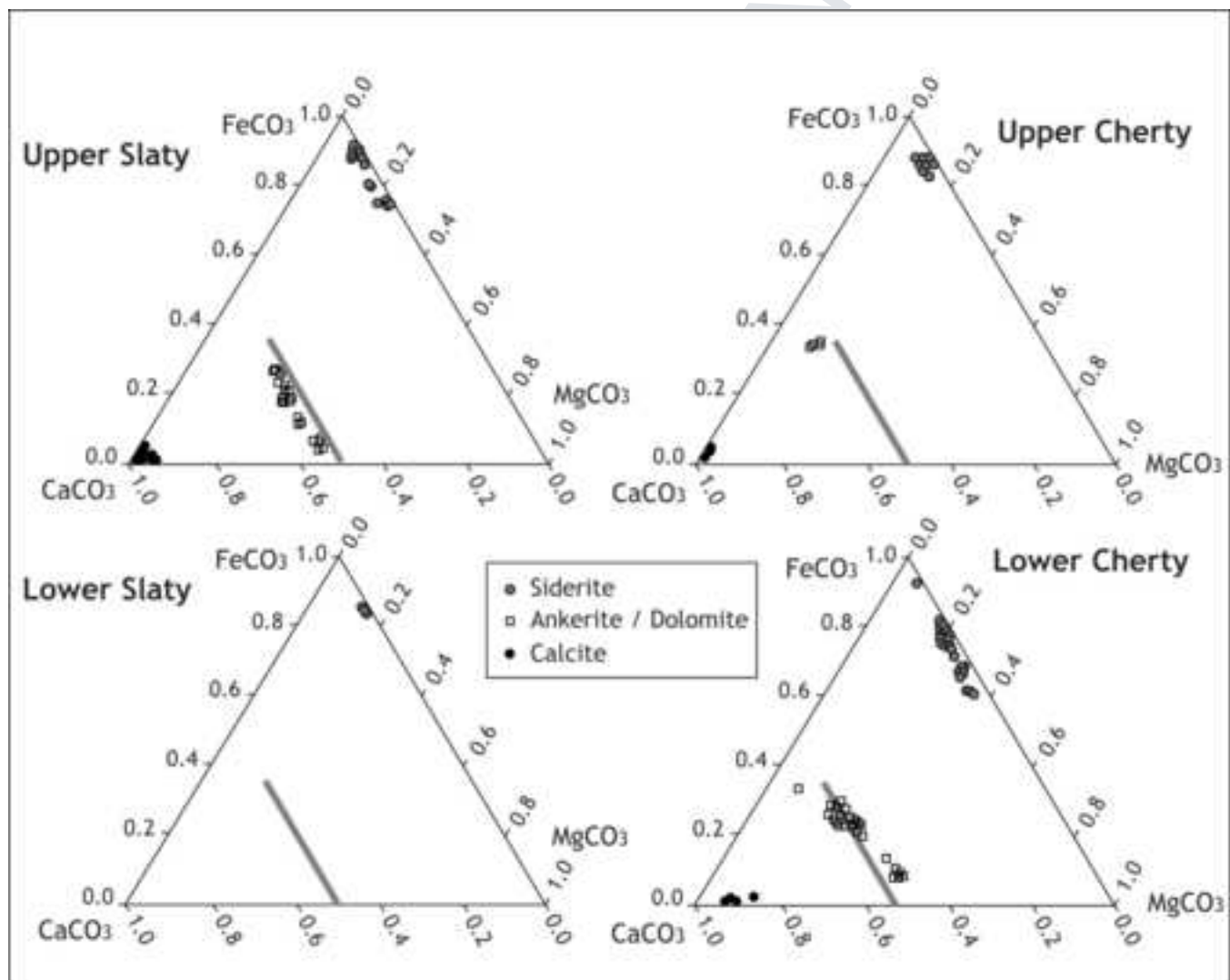
USCRIPT

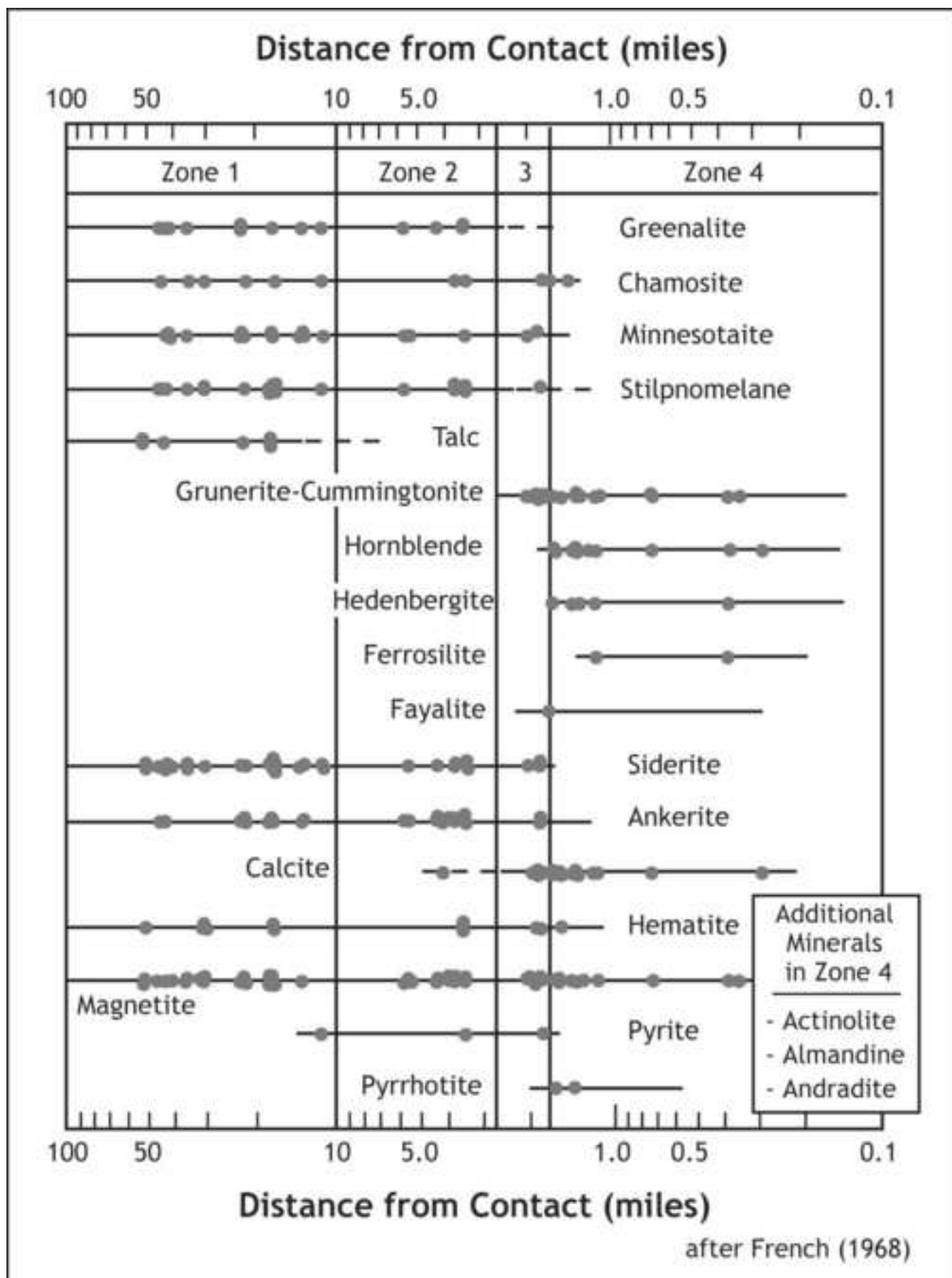


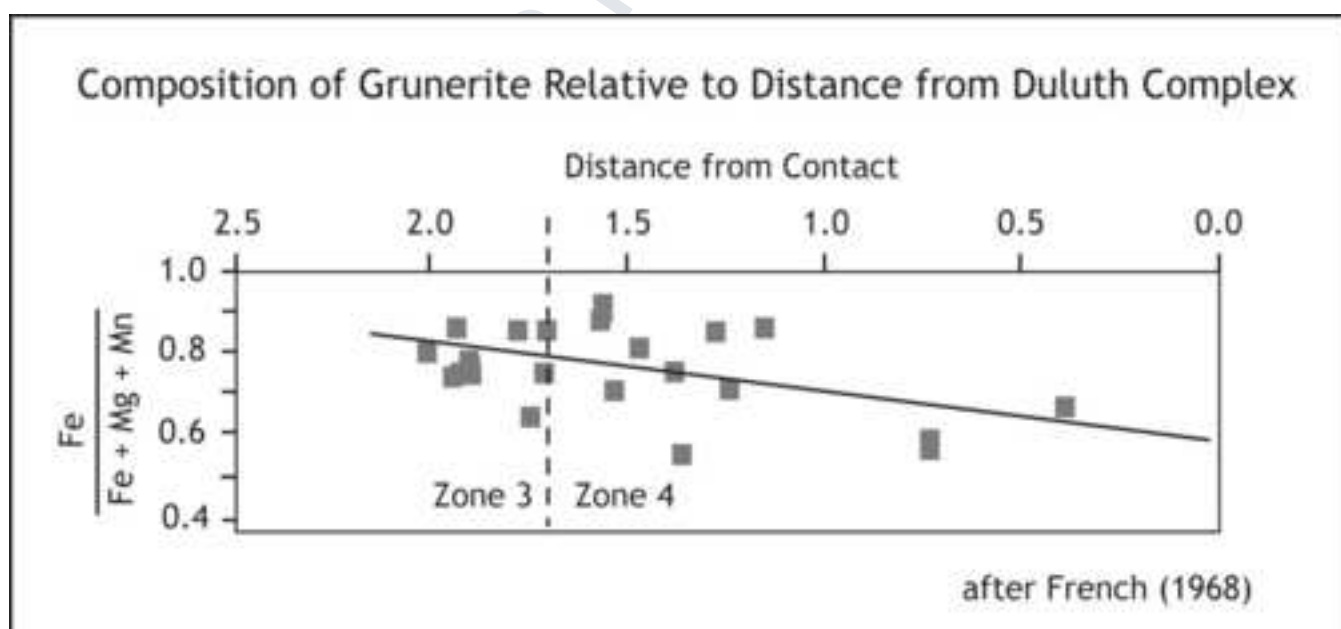


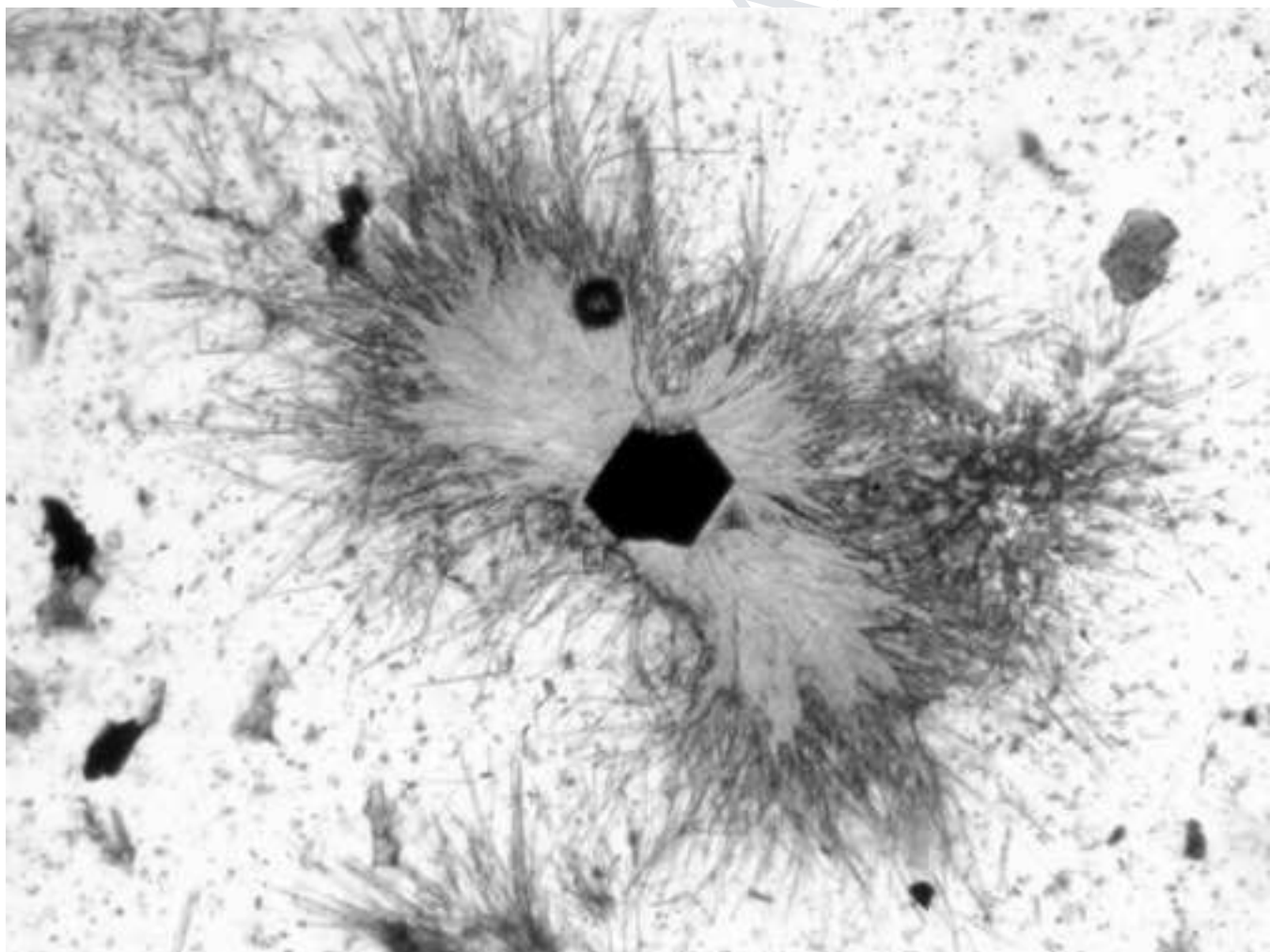


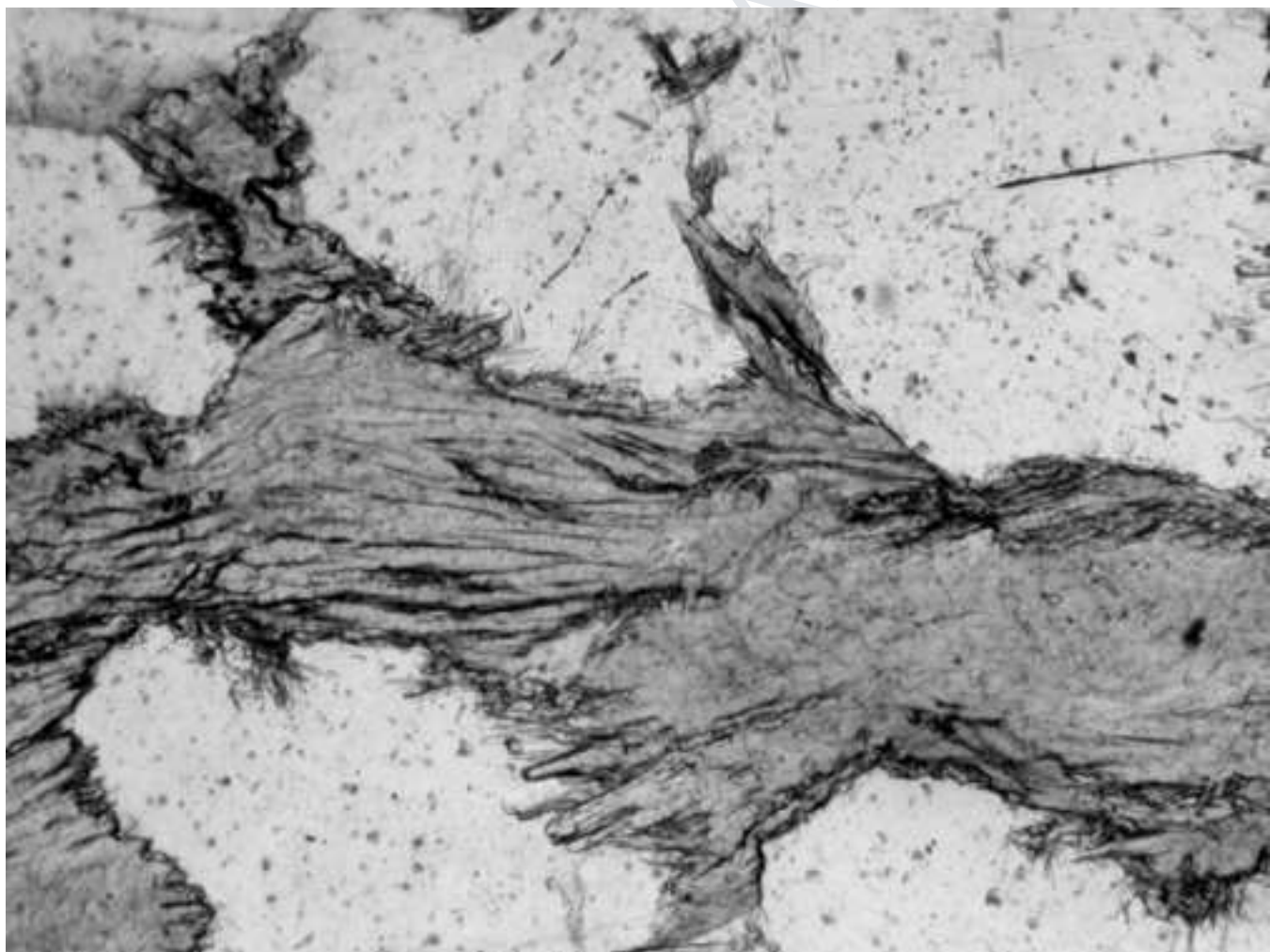




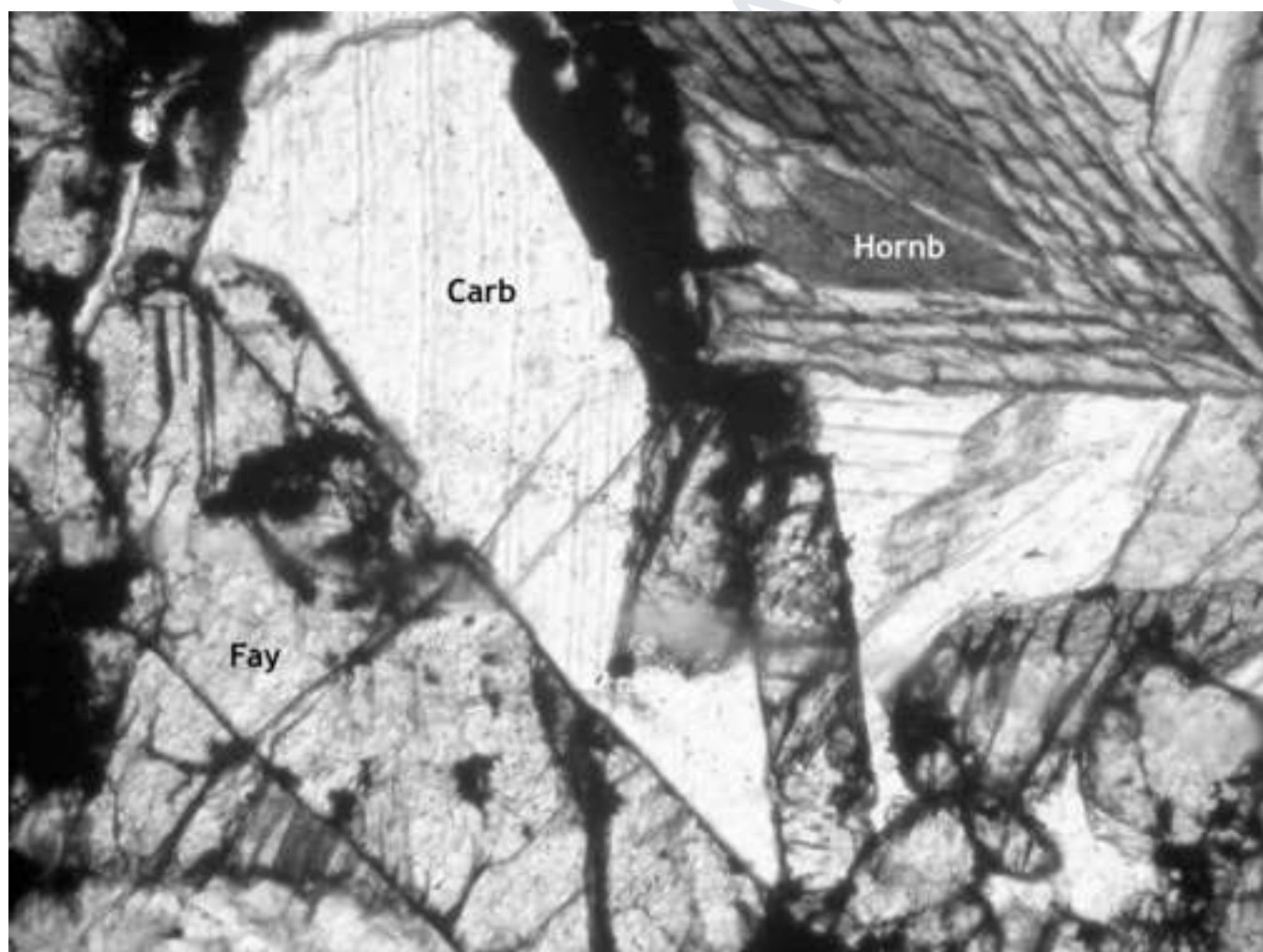


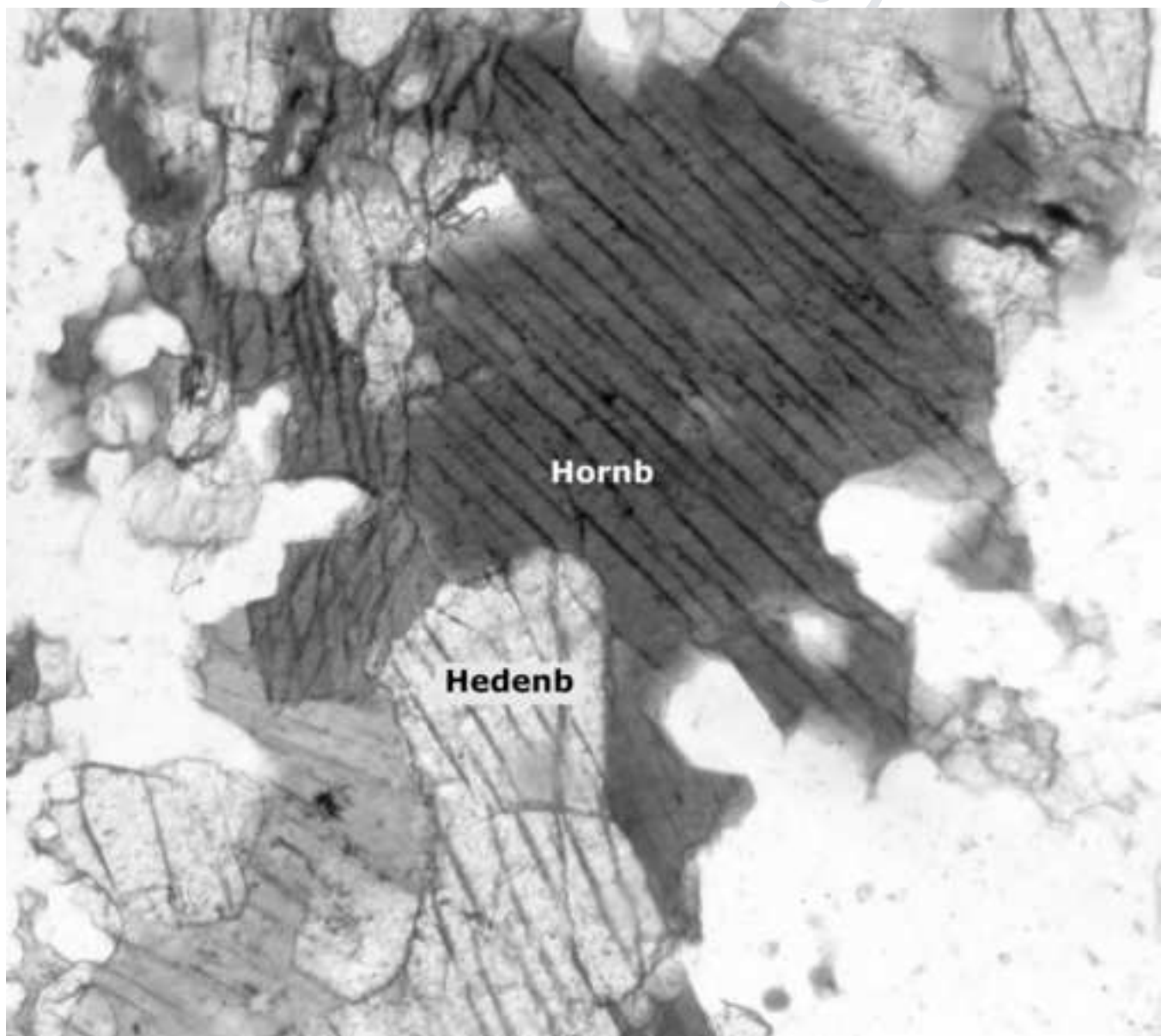






MANUSCRIPT





MANUSCRIPT



